C.P. No. 1282

C.P. No. 1282

PROCUREMENT EXECUTIVE, MINISTRY OF DEFENCE

AERONAUTICAL RESEARCH COUNCIL

CURRENT PAPERS

Free-Stream Turbulence Effects on the Turbulent Boundary Layer

by

R. L. Evans,

SRC Turbomachinery Laboratory,

Cambridge University

LONDON: HER MAJESTY'S STATIONERY OFFICE

1974

PRICE 80p NET

C.P. No.1282*
June, 1973

FREE-STREAM TURBULENCE EFFECTS ON THE TURBULENT BOUNDARY LAYER

- by -
R. L. Evans,≠
SRC Turbomachinery Laboratory,
Cambridge University

SUMMARY

The results of an experimental investigation of the effects of free-stream turbulence on a constant pressure turbulent boundary layer are presented. An increase in the fullness of the velocity profile with a consequent decrease in displacement and momentum thickness and an increase in skin friction is found with increasing free-stream turbulence level. Measurements of some of the turbulence structural properties show an increase in the turbulence kinetic energy and the turbulent shear stress throughout the boundary layer with increasing free-stream turbulence. The turbulent shear stress, $-\rho\,\overline{uv}$, was found to persist into the free-stream, well beyond the usual $\delta_{.99}$ edge of the boundary layer.

---

*Replaces A.R.C.34 586

≠Communicated by Dr. D. S. Whitehead

Free-Stream Turbulence effects on the Turbulent Boundary Layer.

Introduction

In attempts to calculate boundary layers on turbomachine blades the external free-stream conditions become important. In the past, the flow downstream of moving blade rows has been thought of as a highly turbulent one, (Schlichting & Das (1967)). More recent measurements indicate that the flow incident on stator blades should be thought of as both an unsteady and a turbulent flow (Evans (1973). The present experiments were undertaken to gain a clearer understanding of the effects of free-stream turbulence, Tu, on turbulent boundary layer development.

Only a few workers have been interested in the development of turbulent boundary layers under a turbulent free-stream, and there is a lack of reliable data. Kline et al (1960) conducted the first set of experiments designed solely to investigate the effects of increasing Tu on boundary layer growth. They noticed an increase in boundary layer thickness, $\delta_{.99}$ with increasing Tu, and an increased velocity at the "knee" of the profile. They also observed an increase in the skin friction C_f. Robertson and Holt (1972) concentrated their measurements on the skin friction C_f and the shape parameters G and H. They found an increase in C_f and G with increasing Tu, and a decrease in H. The trend was for the change in all these quantities to level off after a Tu level of about 7%.

In a short paper presented at the 1971 AGARD conference on turbulent shear flows, Charnay et al (1971) described some

measurements of a turbulent boundary layer on a flat plate under a turbulent free-stream. They noticed an increase in the skin-friction, the growth rate of the boundary layer and the shear stress at the edge of the layer with increasing Tu. They also found a decrease in the velocity defect profile in the outer part of the layer. Huffman et al (1972) have made a detailed study of the structural properties of the turbulent boundary layer developing under a turbulent free-stream. They have found an increase in the turbulence intensities, turbulent kinetic energy and Reynold's shear stress at the outer edge of the boundary layer with increasing Tu.

Boundary layer calculation methods and free-stream turbulence

At the 1968 Stanford Conference on Turbulent Boundary layer prediction, the method of Bradshaw, Ferris and Atwell (1967) was generally found to be one of the most successful methods. Bradshaw's method solves the momentum equation:

$$U \frac{\partial U}{\partial x} + V \frac{\partial U}{\partial y} = U_\infty \frac{dU_\infty}{dx} + \frac{1}{\rho} \frac{\partial \tau}{\partial y} \qquad (1)$$

The continuity equation:

$$\frac{\partial U}{\partial x} + \frac{\partial V}{\partial y} = 0 \qquad (2)$$

and a transport equation for the turbulent shear stress $\tau = -\rho \overline{uv}$ in equation (1). This equation is derived from the turbulent kinetic energy equation:

$$\tfrac{1}{2}\rho\left(U \frac{\partial \overline{q^2}}{\partial x} + V \frac{\partial \overline{q^2}}{\partial y} \right) - \tau \frac{\partial U}{\partial y} + \frac{\partial}{\partial y}\left(\overline{pv} + \tfrac{1}{2}\rho \overline{q^2 v} \right) + \rho \epsilon = 0 \qquad (3)$$

by assuming that the shear stress τ is directly related to the turbulence kinetic energy $\overline{q^2}/2$. This relationship together with functions relating the diffusion and dissipation terms to the shear stress are determined by empirical observations: $a_1 = \tau/\rho\overline{q^2}$ $\qquad L = \dfrac{(\tau/\rho)^{3/2}}{\epsilon}$

$$G = \left(\frac{\overline{pv}}{\rho} + \tfrac{1}{2}\,\overline{q^2 v}\right) \Big/ \left(\frac{\tau_{max.}}{\rho}\right)^{1/2} \frac{\tau}{\rho}$$

Bradshaw gives G and L as functions of y/δ and quotes a constant value of 0.15 for a_1.

One of the most successful integral boundary layer calculation methods presented at the Stanford Conference was that of Hirst and Reynolds (1968). This method also uses the turbulence kinetic energy equation, but in an integrated form.

The momentum integral equation:

$$\frac{d\theta}{dx} + (H+2)\frac{\theta}{U_\infty}\frac{dU_\infty}{dx} = C_f/2 \qquad (4)$$

is used along with the definition of entrainment:

$$\frac{d}{dx}\int_0^\delta \bar{u}\, dy = E \qquad (5)$$

and the integral turbulence model equation:

$$\frac{d}{dx}\left[\frac{E^2}{2}\int_0^\delta \bar{u}\, dy\right] = K_3\, u_\tau\, E^2 \qquad (6)$$

Equation (6) is the integral of equation (3) from $y=0$ to $y=\delta$ where the entrainment has been linked directly to the turbulence kinetic energy $\overline{q^2}/2$. The

entrainment is taken as $E = K_1 Q$, where Q is a weighted average of $\overline{q^2}$ over the thickness of the boundary layer, and K_1 is some constant.

The constant K_3 is then determined from empirical information, and Hirst and Reynolds quote a value of $K_3 = 0.14$ determined from Wieghardt's flat plate data. These three ordinary differential equations, (4) to (6) together with a skin-friction relation derived from the Coles' (1956) profile are solved using a predictor-corrector technique.

These two calculation procedures, one a differential method and the other an integral method, were considered to be the most suitable for computation of turbulent boundary layers with turbulent free-stream boundaries. The reason for this is that both methods use the turbulent kinetic energy equation to keep track of the turbulence energy within the boundary layer. It should then be possible, by modifying the appropriate boundary conditions, to match the free-stream turbulence energy to the boundary layer turbulence energy at the edge of the layer.

The present experimental program was designed to study the effects of free-stream turbulence on both the integral and structural properties of turbulent boundary layers. Using this information, the modifications necessary for both these methods can then be determined. The actual modifications used, and calculation results, will be detailed in a subsequent report.

Experimental Apparatus

Measurements were made on the boundary layer on the wall of an 8in I.D. perspex pipe at stations 3 ft and 5 ft downstream of the pipe entrance. A contoured inlet section was provided, and a 5/16" diameter trip wire was

glued to the entrance of the pipe. The fan was situated downstream of the test section and the inlet placed in a large settling chamber with a honeycomb and wire gauze at the entrance. A sketch of the tunnel is shown in Fig. 1. Provision was made for placing circular-bar, rectangular mesh grids between the inlet and test section. Only two grids were used, one with 0.25" diameter bars and 1" mesh spacing and one with 0.50" diameter bars and 2" mesh spacing. It was considered that larger diameter bars would provide too much flow blockage and would not yield homogeneous turbulence. The turbulence levels as measured at the pipe centre-line are shown in Fig. 2. A third condition was taken with no grid in place. The turbulence levels on the pipe centre-line at the 3 and 5 ft. stations were 1.0% and 0.6% respectively with no turbulence grids in place.

All boundary layer measurements were made with a linearized DISA hot-wire anemometer. For shear stress measurement and determination of the u and v fluctuations an X-probe was used. A random signal indicator and correlator was used to provide the sum and difference signals necessary to measure shear stress and the individual fluctuating velocities. Appendix A gives details of the X-probe measurements.

The free-stream velocity, U_∞ at the 5 ft. station was set to 50ft/sec. on the pipe centre-line for all measurements. A pitot tube and wall static tapping were used with a micromanometer for this setting. The 99% boundary layer thickness, $\delta_{.99}$ was of the order of 1 in. at the 5ft. station.

Data Reduction and Analysis

All voltages were recorded by hand and converted into velocities by using the appropriate calibration curve obtained beforehand, and the relations given in Appendix A. The hot-wire probes were generally checked for linearization after every three traverses, and the calibration constants set before each traverse.

All mean velocities were plotted against distance from the wall, y, and these values, together with an estimate of the 99% boundary layer thickness, $\delta_{.99}$, fed into a computer program which then generated tables of y, U, y/δ, U/U_∞ and $R_y = \frac{yU_\infty}{\nu}$.

A best fit curve was passed through the data points by hand, and approximately 35 points per profile were read into a second computer program which uses a trapezoidal rule integration scheme to calculate the displacement and momentum thicknesses, δ^* and θ , the shape factor H and the momentum thickness Reynolds number R_θ . For these calculations, no attempt was made to fit a standard sub-layer profile in the region $\frac{yu_\tau}{\nu} = 0$ to $\frac{yu_\tau}{\nu} = 50$ in the manner of Coles (1968), as measurements were made down to $\frac{yu_\tau}{\nu} = 6$ or less, (see Appendix B). Trial calculations were made using Wills' (1962) correction for hot-wire measurements near a wall. There was no change in δ^* and θ to the fourth decimal point, so further corrections were abandoned.

Using the values of U/U_∞ and R_y output from the first program, Clauser plots were formed for each velocity profile to determine the skin-friction C_f. Using this value of C_f and the computed values of δ^* and θ , a third program

was used to calculate Coles' profiles and to generate tables of experimental values of u/u_τ and $\frac{yu_\tau}{\nu}$. Coles (1956) universal turbulent velocity profile is given by:

$$\frac{U}{u_\tau} = \frac{1}{K} \ln \frac{yu_\tau}{\nu} + \frac{\Pi}{K} W(y/\delta) + B \qquad (7)$$

where Π is a parameter and $W(y/\delta)$ is Coles' wake function which can be approximated by:

$$W(y/\delta) = 2 \sin^2\left(\frac{\pi}{2}\frac{y}{\delta}\right) \qquad (8)$$

The Coles' profile may also be written in velocity defect form:

$$\frac{U_\infty - U}{U_\infty} = \frac{\omega}{K}\left\{\Pi\left[2 - W(y/\delta)\right] - \ln(y/\delta)\right\} \qquad (9)$$

$$\omega = \frac{u_\tau}{U_\infty}$$

Using this equation and the definitions of displacement and momentum thicknesses:

$$\delta^* = \int_0^\infty \left(1 - \frac{U}{U_\infty}\right) dy \qquad (10)$$

$$\theta = \int_0^\infty \frac{U}{U_\infty}\left(1 - \frac{U}{U_\infty}\right) dy \qquad (11)$$

and the shape factor $H = \frac{\delta^*}{\theta}$, an equation for Coles' wake parameter Π is found in terms of H and ω.

$$1.5\,\Pi^2 + \left(3.179 - \frac{K}{\omega}\frac{H-1}{H}\right)\Pi + \left(2 - \frac{K}{\omega}\frac{H-1}{H}\right) = 0 \qquad (12)$$

Using the value of ω determined from the Clauser plots and the computed value of H equation (12) is solved for Π. The complete Coles' profile can then be computed to compare with experimental data. The values of Π obtained from

equation (12) and the computed Coles' profiles for all cases are given in Appendix B.

Experimental Results

(I) Integral Properties

All the boundary layer integral parameters were calculated by the method outlined in the previous section. Table 1 gives a summary of the results for three different turbulence levels at positions 3 ft and 5 ft downstream of the trip wire. Fig. 3 shows a typical velocity profile with a best fit curve passed through the experimental points.

The three mean velocity profiles measured at the x = 5 ft. station are shown plotted in dimensional form in Fig. 4. This plot clearly shows the effect of stream turbulence on the profile shape. There appears to be a very slight increase in the 99% boundary layer thickness, δ_{99}, with increasing free-stream turbulence, but there is a marked increase in the "fullness" of the velocity profile. The fuller velocity profiles, if they always had the same δ_{99} would mean a decrease in the displacement and momentum thickness as can be seen from equations (10) and (11). However in the present case there appear to be two conflicting effects, one being the slight increase in δ_{99} tending to increase the integral thicknesses, the other being a "fuller" profile which tends to decrease these thicknesses. Fig. 5 shows the displacement and momentum thickness as a function of free-stream turbulence level. It is seen that the integral thicknesses tend to increase up to a Tu level of approximately 2% and then again start to decrease because of the increasing "fullness" of the velocity profile. Also shown in Fig. 5 is the data of Kline et al (1960) which shows the same trend.

The skin friction for each profile was determined from Clauser plots. Fig. 6 shows the effect of increasing free-stream turbulence on the skin-friction for the profiles measured at the X = 3 ft. station. Also shown on Fig. 6 is the data of Robertson and Holt (1972). For both sets of data the value of C_{f_0} was taken from the formula:

$$C_{f_0} = (4.4 + 3.8 \log R_\theta)^{-2}$$

suggested by Ross (1953). It can be seen that there is a significant increase in skin-friction with increasing free-stream turbulence, leveling off at higher values of Tu. This result is consistent with the fuller velocity profile, which then has a steeper slope at the wall so that the shear stress, τ_w , is higher. The present experiments suggest a greater initial increase in C_f/C_{f_0} with Tu than the data of Robertson and Holt, but tend to level off to the same value. This may be due to the relatively high level of turbulence in the present tunnel with no grids in place.

Using the value of C_f obtained from the Clauser plots and equations (7) and (12), Coles' "law of the wake" velocity profiles were calculated. For these calculations K was taken = 0.41 and B = 5.0 in equation (7). Fig. 7 shows a typical semi-logarithmic velocity profile plot. It is seen from this plot that the first few points measured were just within the viscous sub-layer. This could also be confirmed by observing the hot-wire anemometer signal on an oscilloscope. The outer-layer profiles for three Tu levels are plotted in Fig 8. which indicates that the

Coles' wake component is decreased with increasing Tu. This effect was also noticed by Huffman (1972). That this decreased wake component is due to the fuller velocity profiles can be seen more readily from the velocity defect plots of Fig. 9. Outer layer velocity defect profiles, when made non-dimensional with the friction velocity u_τ are expected to collapse onto a single curve for a constant pressure gradient, as noted by Rotta (1962). It can be seen from Fig. 9 that the outer-layer velocity defect is decreased with increasing Tu. This is consistent with what one would expect from a fuller velocity profile.

II) Turbulence Structural Properties

Figures 10 and 11 show the distribution of the turbulence intensities $\overline{u'^2}/U_\infty^2$ and $\overline{v'^2}/U_\infty^2$ through the boundary layer, for two Tu levels. The longitudinal component is seen to be larger than the transverse component in the inner layer, although the two components converge to the same value at the outer edge of the layer, where the free-stream turbulence is expected to be nearly isotropic. The same data is replotted in Figs 12 and 13 to show the effect of increased Tu on both the longitudinal and transverse fluctuating components. There is a slight increase in intensity in the inner layer with increasing Tu, but a marked increase in the outer layer, no doubt due to the increased mixing with the turbulent free-stream.

In Fig. 14 the distribution of Reynolds shear stress

$$\overline{uv} = -\tau/\rho$$

through the boundary layer is shown for two turbulence levels. There is seen to be an increase in shear stress with increasing free-stream

turbulence which stays more or less constant throughout the boundary layer. With increasing Tu the shear stress is seen to persist further into the free-stream beyond the 99% thickness $\delta_{.99}$.

Twice the turbulence kinetic energy, $\overline{q^2}$, is shown plotted in Fig. 15, where $\overline{q^2} = \overline{u^2} + \overline{v^2} + \overline{w^2}$. For these plots, the $\overline{w^2}$ component, which was not measured, was taken to be $1.2\,\overline{v^2}$ following Huffman (1972). Again there is seen to be a slight increase in turbulence kinetic energy in the inner layer, with a much greater increase in the outer mixing layer due to increased Tu. The ratio of Reynolds shear stress to turbulence kinetic energy is shown in Fig. 16. This quantity is a_1 which Bradshaw et al. (1967) take as a constant 0.15 in their calculation method. At the lower turbulence level, the peak value is very near 0.15 and is somewhat higher with increased free-stream turbulence. In both cases the ratio falls off rapidly after the peak which occurs just outside the sub-layer.

Conclusions

The effects of increasing free-stream turbulence Tu on the turbulent boundary layer can be summarized as follows:

(1) An increase at first, and then decrease in the displacement and momentum thicknesses δ^* and θ. These increase at first due to a slight increase in $\delta_{.99}$ and then decrease due to a fuller velocity profile.

(2) An increase in the skin friction, C_f. This is consistent with a fuller velocity profile and hence an increasing gradient $\frac{\partial U}{\partial y}$ at the wall.

(3) A decrease in the wake component of the Coles' profile and the outer layer velocity defect, which indicates a departure from the "universal" law of the wake in the outer layer.

(4) An increase in turbulence intensities and kinetic energy, especially in the outer mixing region where the flow interacts with the free stream.

(5) An increase in turbulent shear stress, $-\rho\overline{uv}$, and a continuation of the shear stress past the 99% "edge" of the boundary layer.

(6) An increase in the ratio of turbulent shear stress to kinetic energy, a_1.

Nomenclature.

a_1 - Ratio of shear stress to turbulence kinetic energy; constant in Bradshaw's calculation scheme.

B - Constant in the law of the wall = 5.0

C_f - Skin friction coefficient =

E - Entrainment

G - Shape factor = $\frac{\delta}{\theta}$; Bradshaw's diffusion term

H - Shape factor = $\frac{\delta^*}{\theta}$

K - Constant in the law of the wall = 0.41

L - Bradshaw's dissipation function

Q - Velocity scale in Hirst and Reynold's calculation scheme $Q^2 = \frac{\int_0^\delta \bar{u}\,\overline{q^2}\,dy}{\int_0^\delta \bar{u}\,dy}$

$\overline{q^2}$ - Twice the turbulence kinetic energy

R_y - Local Reynolds No. = $\frac{y U_\infty}{\nu}$

R_θ - Momentum thickness Reynolds No. = $\frac{\theta U_\infty}{\nu}$

Tu - Free-stream turbulence level = $\frac{\sqrt{\overline{u'^2}}}{U_\infty}$

U - Mean velocity in X direction

U_∞ - Free-stream velocity

u', v', w' - Turbulent fluctuating velocities

$\tilde{u}, \tilde{v}, \tilde{w}$ - Root-mean-square values of the fluctuating velocities

X - Distance from the pipe entrance

δ_{99} - Boundary layer 99% thickness

δ^* - Boundary layer displacement thickness

Π - Parameter in Coles' law of the wake

ω - Dimensionless friction velocity = u_τ / U_∞

τ_w - Wall shearing stress

θ - Boundary layer momentum thickness

u_τ - Friction velocity $= \sqrt{\tau_w/\rho}$

ρ - Fluid density

ν - Kinematic viscosity

References

No.	Author(s)	Title, etc.
1	P. Bradshaw, D. H. Ferris and N. P. Atwell	Calculation of boundary layer development using the turbulent energy equation. J.F.M. 28, pt. III, pp.593-616. 1967.
2	G. Charnay, G. Comte-Bellot and J. Mathieu	Development of a turbulent boundary layer on a flat plate in an external turbulent flow. AGARD CPP 93-71. 1971.
3	D. Coles	The law of the wake in the turbulent boundary layer. J.F.M. 1, pp.191-226. 1956.
4	D. Coles	The young person's guid to the data. Proceedings AFOSR-IFP-STANFORD 1968 Conference on Turbulent Boundary Layer Prediction, Vol.2. 1968.
5	R. L. Evans	Turbulence and unsteadiness measurements downstream of a moving blade row. Cambridge University Turbo. Rpt. CUED/A Turbo/TR 47. 1973.
6	E. A. Hirst and W. C. Reynolds	An integral prediction method for turbulent boundary layers using the turbulent kinetic energy equation. Stanford Report MD-21. 1968.
7	G. D. Huffman, D. R. Zimmerman and W. A. Bennet	The effect of free-stream turbulence level on turbulent boundary layer behaviour. AGARD paper presented at Paris Turbomachinery Meeting, April, 1972. 1972.
8	R. Kiock	Turbulence downstream of stationary and rotating cascades. ASME Paper 73-GT-80. 1972.
9	S. J. Kline, A. V. Lisin and B. A. Waitman	Preliminary experimental investigation of effect of free-stream turbulence on turbulent boundary layer growth. NASA TN D-368. 1960.
10	C. J. Lawn	Turbulence measurements with hot-wires at BNL. CEGB Report RD/B/M1277. 1969.

11/

No.	Author(s)	Title, etc.
11	J. M. Robertson and C. F. Holt	Stream turbulence effects on the turbulent boundary layer. Submitted to the proceedings of the ASCE. 1972.
12	D. Ross	A new analysis of Nikuradse experiments on turbulent flow in smooth pipes. Proc. 3rd Midwest Conference on Fluid Mechanics. 1953.
13	J. C. Rotta	Turbulent boundary layers in incompressible flow. Progress in Aero. Sciences, Vol.2. 1962
14	H. Schlichting and A. Das	On the influence of turbulence level on the aerodynamic losses of axial turbomachines. in Flow Research on Blading ed. L. S. Dzung, Elsevier Publishing Co. 1970.
15	J. A. B. Wills	The correction of hot-wire readings for promimity to a solid boundary. J.F.M. 12, pp.388-396. 1962.

APPENDIX A

Turbulence Measurements with a hot-wire Anemometer X-probe

All the turbulence measurements reported in this paper, with the exception of the mean flow velocities were made with an X-probe. The development of the necessary equations, and the notation closely follows that given by Lawn (1969).

A single hot-wire, exposed to an air flow will respond with a voltage,

$$\frac{V^2}{R_w(R_w-R_g)} = A + B\,U_{eff.}^{0.45} \qquad (1)$$

where Rw = resistance at wire temp

Rg = resistance at ambient temp

U_{eff} is the effective cooling velocity. If the hot-wire probe lies in the X-Y plane of Fig. A-1, with the wire normal to the X direction, U_{eff} can be given by:

$$U_{eff}^2 = U^2 + K_1^2 V^2 + K_2^2 W^2 \qquad (2)$$

We now consider a flow with mean velocity $\bar{U}$ in the X direction and turbulent fluctuating velocities u, v and w. For a probe held in the mean flow direction, but with a wire held at an angle ($\pi/2 - \phi$) to this direction, as in Fig. A-2, U_{eff} is given by:

$$U_{eff}^2 = \left\{(\bar{U}+u)\cos\phi + v\sin\phi\right\}^2$$

$$+ K_1^2\left\{(\bar{U}+u)\sin\phi - v\cos\phi\right\}^2 + K_2^2 w^2 \qquad (3)$$

To first order in the fluctuating components, and taking time means noting that $\bar{u} = \bar{v} = \bar{w} = 0$,

$$\bar{U}_{eff} = \bar{U} \left(\cos^2 \phi + K_1^2 \sin^2 \phi\right)^{1/2} \quad (4)$$

In hot wire anemometry it is usual to linearize the signal, so that eq'n (1) becomes,

$$V = D + C\, U_{eff} \quad (5)$$

The slope of the calibration curve is then

$$C = \frac{d\bar{V}}{dU_{eff}}$$

where $\bar{V}$ is the time mean or D.C. voltage.

Then, from eq'n (4)

$$C = \frac{d\bar{V}}{d\bar{U}} \left(\cos^2 \phi + K_1^2 \sin^2 \phi\right)^{-1/2} \quad (6)$$

Expanding eq'n (3) and taking 1st order terms only

$$U_{eff} = \bar{U} \left(\cos^2 \phi + K_1^2 \sin^2 \phi\right)^{1/2} \left\{ 1 + \frac{u}{\bar{U}} + \frac{v}{\bar{U}} \frac{\cos \phi \sin \phi \,(1 - K_1^2)}{\cos^2 \phi + K_1^2 \sin^2 \phi} \right\} \quad (7)$$

It can now be seen that a single wire normal to the mean flow will yield a fluctuating signal,

$$V' = C\, u \quad (8)$$

A X-probe, with the two wires at $+\pi/4$ and $-\pi/4$ to the flow direction will yield the two fluctuating signals,

$$V_1' = C_1 \left\{ u + v \left(\frac{1 - K_1^2}{1 + K_1^2} \right) \right\} \quad (9)$$

$$V_2' = C_2 \left\{ u - v \left(\frac{1 - K_1^2}{1 + K_1^2} \right) \right\} \quad (10)$$

When linearizing the two wires, it is usual to adjust the linearizing circuits so that $C_1 = C_2 = C$
If this is done, the sum and difference ofthe signals measured with an rms voltmeter are

$$\widetilde{V}_{1+2} = 2 C \tilde{u} \quad (11)$$

$$\widetilde{V}_{1-2} = 2 C \tilde{v} \left(\frac{1 - K_1^2}{1 + K_1^2} \right) \quad (12)$$

These two equations form the basis of all the X-probe measurements. The value for the constant in eq'n (12) was taken to be $K_1 = 0.23$ as given by Lawn.

In order to measure the turbulent shear stress, $-\rho \overline{uv}$ the ratio $R_{\overline{uv}} = \frac{\overline{uv}}{\tilde{u}\tilde{v}}$ is obtained directly from a DISA signal correlator. The $\tilde{u}$ and $\tilde{v}$ values are taken from eq'ns (11) and (12) so that:

$$-\rho \overline{uv} = -\rho \frac{\widetilde{V}_{1+2} \, \widetilde{V}_{1-2}}{4 C^2 \left(\frac{1 - K_1^2}{1 + K_1^2} \right)} R_{\overline{uv}} \quad (13)$$

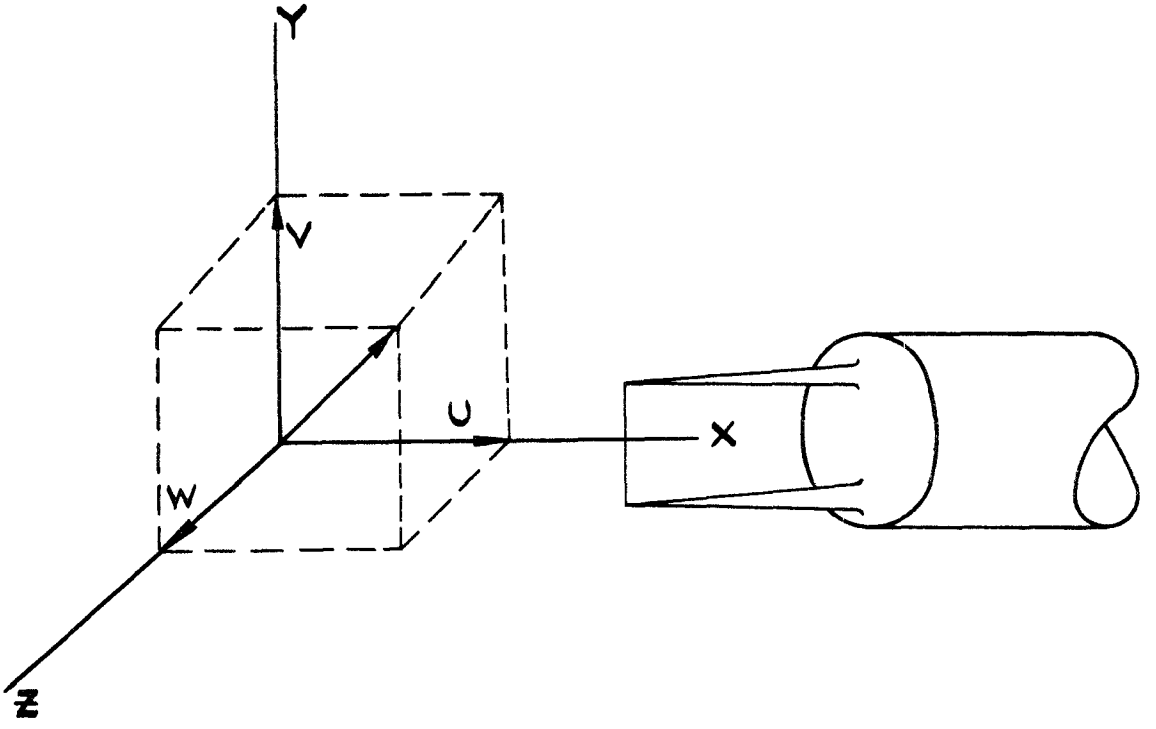

FIG. A-1

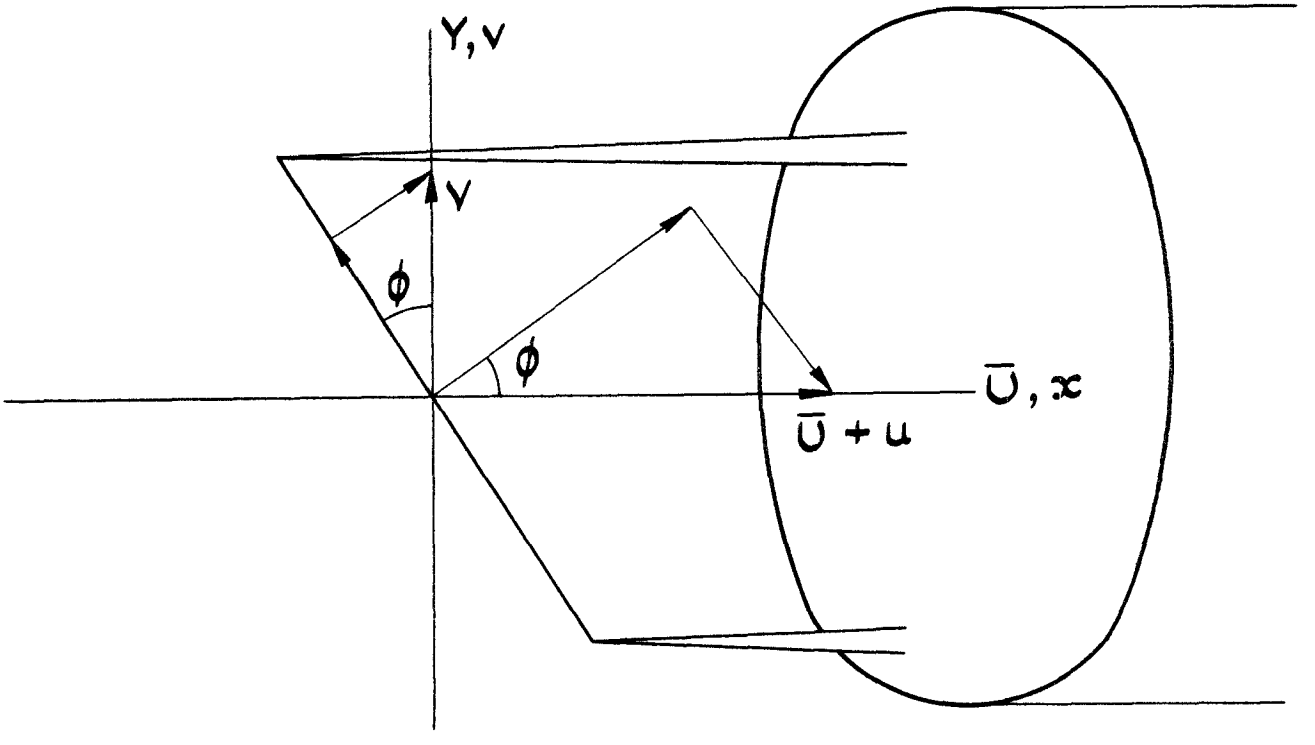

FIG. A-2.

APPENDIX B

This appendix gives the experimental values for all the mean velocity profiles measured, together with values for a Coles' velocity profile calculated from equation (7). The value of Π used in these calculations is obtained from equation (12) and is listed for each profile.

RUN NO. 36 X=3.0 FT. U1= 50.00 FT./SEC.

0.0 IN. TURBULENCE GRID

CF=.0038

DELTA=0.900 IN.

DELTA*=.0871 IN.

THETA=.0651 IN.

Y/DELTA	U/U1	Y*UTAU/NU	U/UTAU EXP.	U/UTAU COLES
0.0056	0.260	5.660	5.965	9.228
0.0111	0.450	11.320	10.324	10.919
0.0167	0.566	16.979	12.985	11.908
0.0222	0.620	22.639	14.224	12.611
0.0278	0.654	28.299	15.004	13.156
0.0333	0.670	33.959	15.371	13.602
0.0389	0.680	39.619	15.600	13.979
0.0444	0.686	45.279	15.738	14.307
0.0500	0.690	50.938	15.830	14.596
0.0556	0.696	56.598	15.967	14.855
0.0667	0.706	67.918	16.197	15.305
0.0778	0.714	79.238	16.380	15.686
0.0889	0.722	90.557	16.564	16.019
0.1000	0.732	101.877	16.793	16.31[illegible]
0.1111	0.742	113.196	17.083	16.57[illegible]
0.1222	0.754	124.516	17.298	16.820
0.1389	0.774	141.496	17.757	17.147
0.1667	0.804	169.795	18.445	17.621
0.1944	0.832	198.094	19.087	18.032
0.2222	0.850	226.393	19.500	18.396
0.2778	0.876	282.991	20.097	19.031
0.3333	0.896	339.589	20.556	19.580
0.3889	0.916	396.188	21.014	20.071
0.4444	0.934	452.786	21.427	20.520
0.5000	0.950	509.384	21.794	20.934
0.5556	0.962	565.982	22.070	21.318
0.6111	0.972	622.581	22.299	21.674
0.6667	0.980	679.179	22.483	22.002
0.7222	0.984	735.777	22.575	22.302
0.7778	0.990	792.375	22.712	22.572
0.8333	0.992	848.974	22.758	22.814
0.8889	0.998	905.572	22.896	23.025
1.0000	1.000	1018.768	22.942	23.357

NU= 1.6045X 10-4 UTAU= 2.1794

PI= 0.2999

RUN NO. 35 X=3.0 FT. U1= 50.00 FT./SEC.

.25 IN. TURBULENCE GRID

CF=.0040

DELTA=1.050 IN.

DELTA*=.1051 IN.

THETA=.0814 IN.

Y/DELTA	U/U1	Y*UTAU/NU	U/UTAU EXP.	U/UTAU COLES
0.0048	0.260	5.807	5.814	9.290
0.0095	0.460	11.614	10.286	10.981
0.0143	0.574	17.421	12.835	11.970
0.0190	0.610	23.227	13.640	12.672
0.0238	0.640	29.034	14.311	13.216
0.0286	0.656	34.841	14.669	13.661
0.0333	0.668	40.648	14.937	14.037
0.0381	0.680	46.455	15.205	14.363
0.0476	0.696	58.069	15.563	14.908
0.0571	0.712	69.682	15.921	15.353
0.0714	0.730	87.103	16.323	15.899
0.0952	0.758	116.137	16.949	16.603
0.1190	0.780	145.171	17.441	17.151
0.1429	0.800	174.206	17.889	17.600
0.1667	0.816	203.240	18.246	17.980
0.1905	0.830	232.274	18.559	18.311
0.2381	0.854	290.343	19.096	18.869
0.2857	0.876	348.411	19.588	19.328
0.3333	0.896	406.480	20.035	19.721
0.3810	0.912	464.549	20.393	20.065
0.4286	0.924	522.617	20.661	20.372
0.4762	0.936	580.686	20.930	20.650
0.5238	0.946	638.754	21.153	20.903
0.5714	0.952	696.823	21.287	21.135
0.6190	0.958	754.891	21.422	21.350
0.6667	0.964	812.960	21.556	21.549
0.7619	0.974	929.097	21.779	21.907
0.8571	0.986	1045.234	22.048	22.217
0.9524	0.990	1161.371	22.137	22.486
1.0476	1.000	1277.508	22.361	22.719

NU= 1.6045X 10-4 UTAU= 2.2361

PI= 0.0563

RUN NO. 30 X=3.0 FT. U1= 50.00 FT./SEC.

.50 IN. TURBULENCE GRID

CF=.0042

DELTA=1.130 IN.

DELTA*=.0916 IN.

THETA=.0704 IN.

Y/DELTA	U/U1	Y*UTAU/NU	U/UTAU EXP.	U/UTAU COLES
0.0044	0.300	5.753	6.547	9.268
0.0088	0.500	11.505	10.911	10.958
0.0133	0.576	17.258	12.569	11.947
0.0177	0.614	23.011	13.399	12.649
0.0221	0.634	28.764	13.835	13.193
0.0265	0.654	34.516	14.271	13.638
0.0310	0.672	40.269	14.664	14.014
0.0354	0.686	46.022	14.970	14.340
0.0442	0.706	57.527	15.406	14.885
0.0531	0.724	69.032	15.799	15.330
0.0619	0.740	80.538	16.148	15.707
0.0708	0.750	92.043	16.366	16.033
0.0885	0.766	115.054	16.715	16.580
0.1106	0.780	143.818	17.021	17.127
0.1327	0.806	172.581	17.588	17.575
0.1549	0.830	201.345	18.112	17.956
0.1770	0.846	230.108	18.461	18.086
0.1991	0.860	258.872	18.767	18.579
0.2212	0.870	287.635	18.985	18.842
0.2434	0.880	316.399	19.203	19.082
0.2655	0.892	345.162	19.465	19.301
0.3097	0.910	402.689	19.858	19.693
0.3540	0.926	460.216	20.207	20.036
0.3982	0.940	517.744	20.512	20.341
0.4425	0.954	575.271	20.818	20.618
0.4867	0.964	632.798	21.036	20.870
0.5310	0.970	690.325	21.167	21.102
0.5752	0.976	747.852	21.298	21.317
0.6195	0.980	805.379	21.385	21.517
0.7080	0.986	920.433	21.516	21.878
0.7965	0.992	1035.487	21.647	22.193
0.8850	0.998	1150.541	21.778	22.469
0.9735	1.000	1265.595	21.822	22.710

NU= 1.6596X 10-4 UTAU= 2.2913

PI= 0.0591

RUN NO. 15 X=5.0 FT. U1= 50.00 FT./SEC.

0.0 IN. TURBULENCE GRID

CF=.0037

DELTA=1.330 IN.

DELTA*=.1649 IN.

THETA=.1250 IN.

Y/DELTA	U/U1	Y*UTAU/NU	U/UTAU EXP.	U/UTAU COLES
0.0038	0.250	5.626	5.812	9.213
0.0053	0.350	7.876	8.137	10.034
0.0075	0.450	11.251	10.462	10.904
0.0113	0.524	16.877	12.183	11.893
0.0150	0.556	22.503	12.927	12.595
0.0183	0.580	28.128	13.485	13.139
0.0226	0.600	33.754	13.960	13.584
0.0301	0.614	45.005	14.275	14.287
0.0376	0.642	56.256	14.926	14.833
0.0451	0.658	67.508	15.298	15.279
0.0526	0.670	78.759	15.577	15.657
0.0602	0.684	90.010	15.903	15.985
0.0752	0.696	112.513	16.182	16.534
0.0940	0.714	140.641	16.600	17.087
0.1316	0.746	196.898	17.344	17.929
0.1692	0.774	253.154	17.995	18.570
0.2068	0.798	309.411	18.553	19.094
0.2444	0.826	365.667	19.065	19.542
0.2820	0.840	421.924	19.530	19.937
0.3195	0.850	478.180	19.902	20.293
0.3571	0.870	534.437	20.227	20.618
0.3947	0.880	590.693	20.460	20.920
0.4323	0.888	646.950	20.646	21.201
0.4699	0.896	703.206	20.832	21.466
0.5075	0.904	759.462	21.018	21.716
0.5451	0.914	815.719	21.250	21.952
0.6203	0.932	928.232	21.669	22.387
0.6955	0.950	1040.745	22.087	22.776
0.7707	0.974	1153.258	22.645	23.118
0.8459	0.986	1265.771	22.924	23.416
0.9211	0.998	1378.284	23.203	23.668
0.9962	1.000	1490.797	23.250	23.875

NU= 1.5928X 10-4 UTAU= 2.1506

PI= 0.2159

RUN NO. 18 X=5.0 FT. U1= 50.00 FT./SEC.

.25 IN. TURBULENCE GRID

CF=.0038

DELTA=1.450 IN.

DELTA*=.1650 IN.

THETA=.1274 IN.

Y/DELTA	U/U1	Y*UTAU/NU	U/UTAU EXP.	U/UTAU COLES
0.0034	0.230	5.651	5.277	9.224
0.0048	0.300	7.912	6.832	10.045
0.0069	0.400	11.303	9.177	10.915
0.0103	0.516	16.954	11.838	11.904
0.0138	0.550	22.606	12.618	12.606
0.0172	0.576	28.257	13.214	13.150
0.0207	0.594	33.909	13.627	13.595
0.0276	0.618	45.212	14.178	14.297
0.0345	0.640	56.515	14.683	14.842
0.0414	0.654	67.818	15.004	15.287
0.0483	0.670	79.120	15.371	15.664
0.0552	0.680	90.423	15.600	15.991
0.0690	0.702	113.089	16.105	16.538
0.0862	0.724	141.287	16.610	17.086
0.1034	0.744	169.544	17.069	17.535
0.1207	0.760	197.801	17.436	17.916
0.1552	0.786	254.316	18.032	18.542
0.1897	0.810	310.830	18.583	19.048
0.2241	0.826	367.345	18.950	19.474
0.2586	0.844	423.860	19.363	19.845
0.2931	0.862	480.374	19.776	20.174
0.3276	0.876	536.889	20.097	20.471
0.3621	0.890	593.403	20.418	20.743
0.3966	0.902	649.918	20.693	20.994
0.4310	0.910	706.433	20.877	21.227
0.4655	0.920	762.947	21.106	21.446
0.5000	0.926	819.462	21.244	21.651
0.5690	0.938	932.491	21.519	22.028
0.6379	0.950	1045.520	21.794	22.366
0.7069	0.960	1158.550	22.024	22.670
0.7759	0.968	1271.579	22.207	22.942
0.8448	0.976	1384.608	22.391	23.185
0.9138	0.986	1497.637	22.620	23.400
0.9828	0.990	1610.667	22.712	23.587
1.0517	0.992	1723.696	22.758	23.749

NU= 1.6068X 10-4 UTAU= 2.1794

PI= 0.1183

RUN NO. 25 X=5.0 FT. U1= 50.00 FT./SEC.

.50 IN. TURBULENCE GRID

CF=.0039

DELTA=1.200 IN.

DELTA*=.1183 IN.

THETA=.0886 IN.

Y/DELTA	U/U1	Y*UTAU/NU	U/UTAU EXP.	U/UTAU COLES
0.0042	0.260	5.608	5.888	9.205
0.0058	0.350	7.851	7.926	10.026
0.0083	0.450	11.216	10.190	10.896
0.0125	0.530	16.825	12.002	11.885
0.0167	0.574	22.433	12.999	12.588
0.0208	0.604	28.041	13.678	13.132
0.0250	0.620	33.649	14.040	13.578
0.0292	0.628	39.257	14.221	13.954
0.0333	0.636	44.865	14.403	14.281
0.0375	0.642	50.474	14.538	14.569
0.0417	0.650	56.082	14.720	14.827
0.0500	0.664	67.298	15.037	15.274
0.0583	0.676	78.514	15.308	15.653
0.0667	0.686	89.731	15.535	15.982
0.0750	0.698	100.947	15.807	16.273
0.0833	0.706	112.163	15.988	16.534
0.1042	0.730	140.204	16.531	17.091
0.1250	0.752	168.245	17.029	17.550
0.1458	0.770	196.286	17.437	17.944
0.1667	0.790	224.327	17.890	18.289
0.2083	0.824	280.408	18.660	18.881
0.2500	0.854	336.490	19.339	19.381
0.2917	0.882	392.572	19.973	19.821
0.3333	0.904	448.654	20.472	20.217
0.3750	0.922	504.735	20.879	20.580
0.4167	0.936	560.817	21.196	20.918
0.4583	0.948	616.899	21.468	21.233
0.5000	0.956	672.980	21.649	21.530
0.5417	0.962	729.062	21.785	21.810
0.5833	0.968	785.144	21.921	22.074
0.6250	0.972	841.225	22.011	22.322
0.7083	0.980	953.389	22.193	22.774
0.7917	0.986	1065.552	22.329	23.165
0.8750	0.994	1177.716	22.510	23.493
0.9583	0.998	1289.879	22.600	23.759
1.0417	1.000	1402.042	22.646	23.962

NU= 1.6404X 10-4 UTAU= 2.2079

PI= 0.2656

X = 5ft. Rx = 1.5 x 10^6

	No Grid	¼" Grid	½" Grid
Tu%	0.6	1.39	2.38
C_f	.0037	.0038	.0039
δ^*	.1640 in	.1650 in	.1183in
θ	.1250in	.1274 in	.0886in
H	1.31	1.30	1.34
δ	1.330 in	1.450 in	1.200 in
R_θ	3271	3304	2249

X = 3ft. Rx = 0.9 x 10^6

	No Grid	¼" Grid	½" Grid
Tu%	1.0	1.94	3.42
C_f	.0038	.0040	.0042
δ^*	.0871 in	.1051 in	.0916 in
θ	.0651 in	.0814 in	.0704 in
H	1.34	1.29	1.30
δ	0.900 in	1.050 in	1.130in
R_θ	1690	2113	1760

TABLE I

Summary of Integral Results.

Produced in England by Her Majesty's Stationery Office, Reprographic Centre, Basildon

R 74413/R54 425 2/74 P

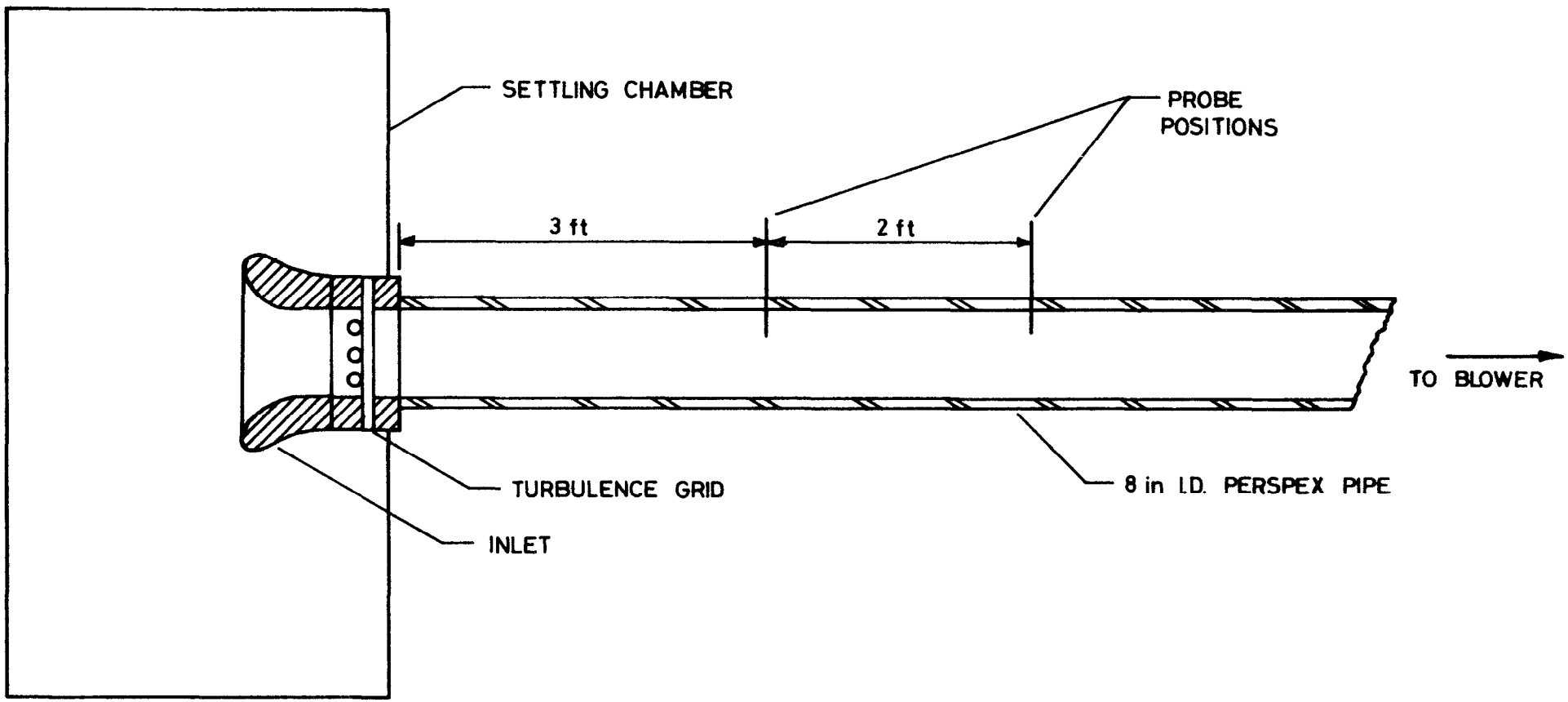

FIG. 1, TUNNEL SCHEMATIC

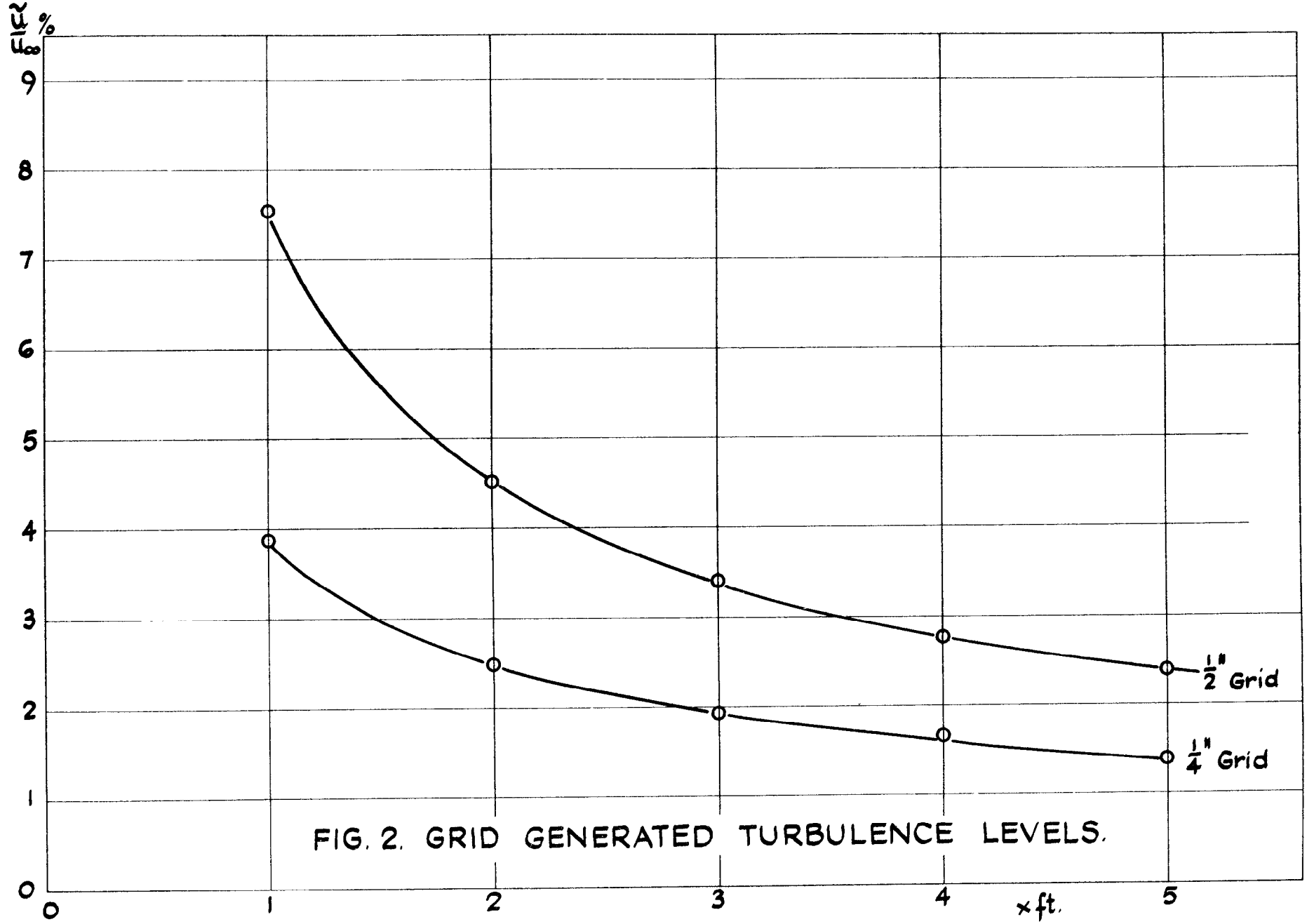

FIG. 2. GRID GENERATED TURBULENCE LEVELS.

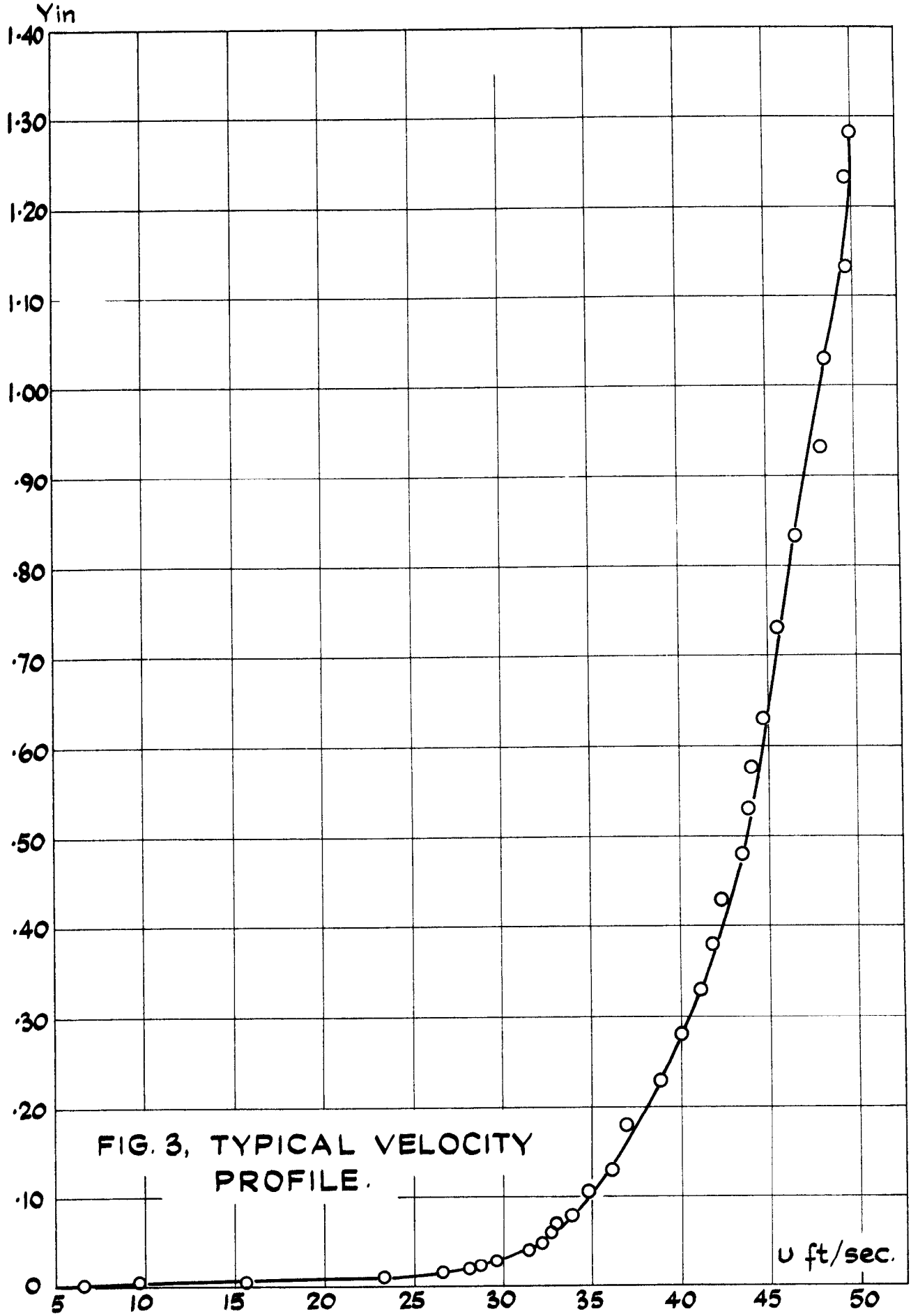

FIG. 3, TYPICAL VELOCITY PROFILE.

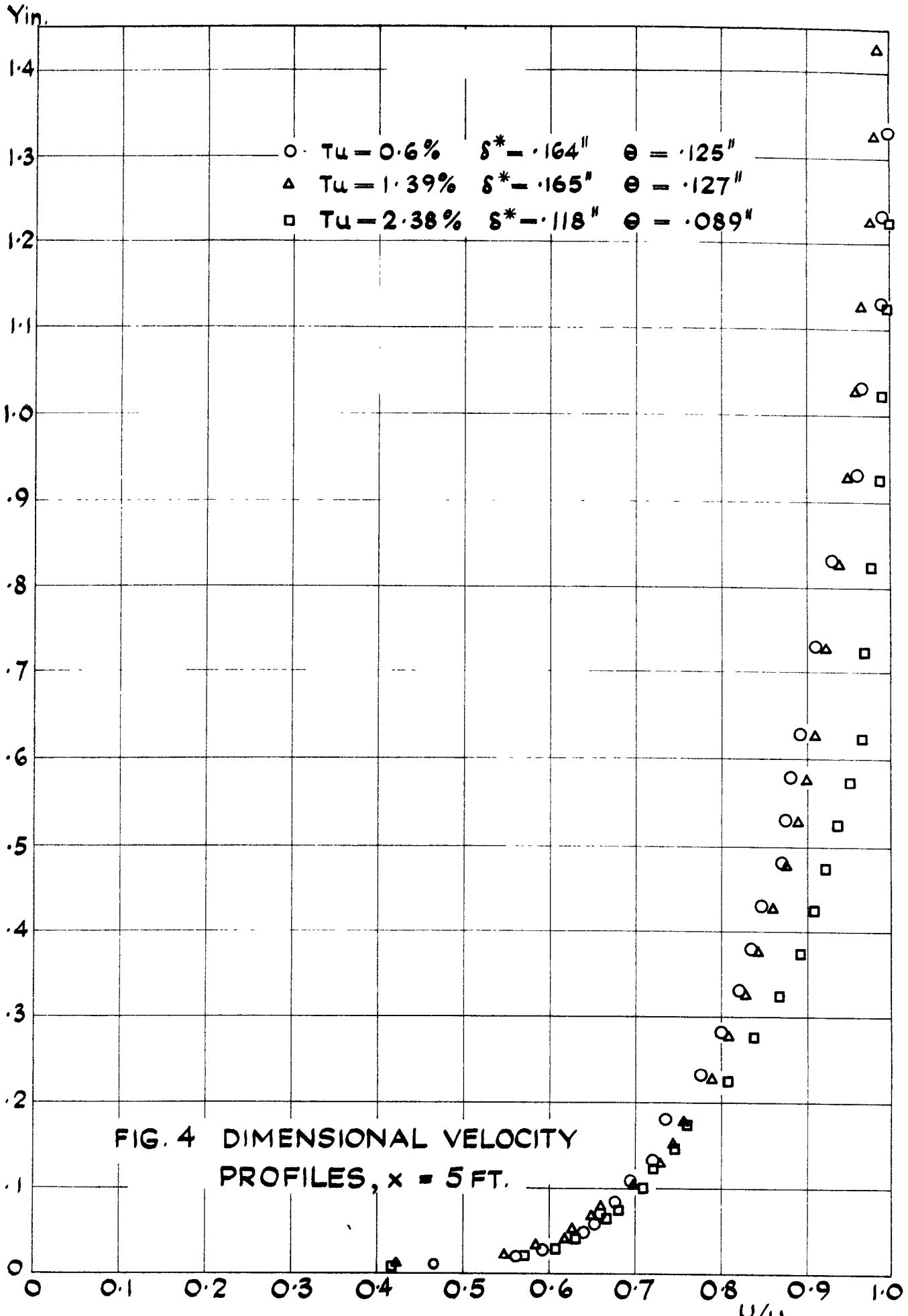

FIG. 4 DIMENSIONAL VELOCITY PROFILES, x = 5 FT.

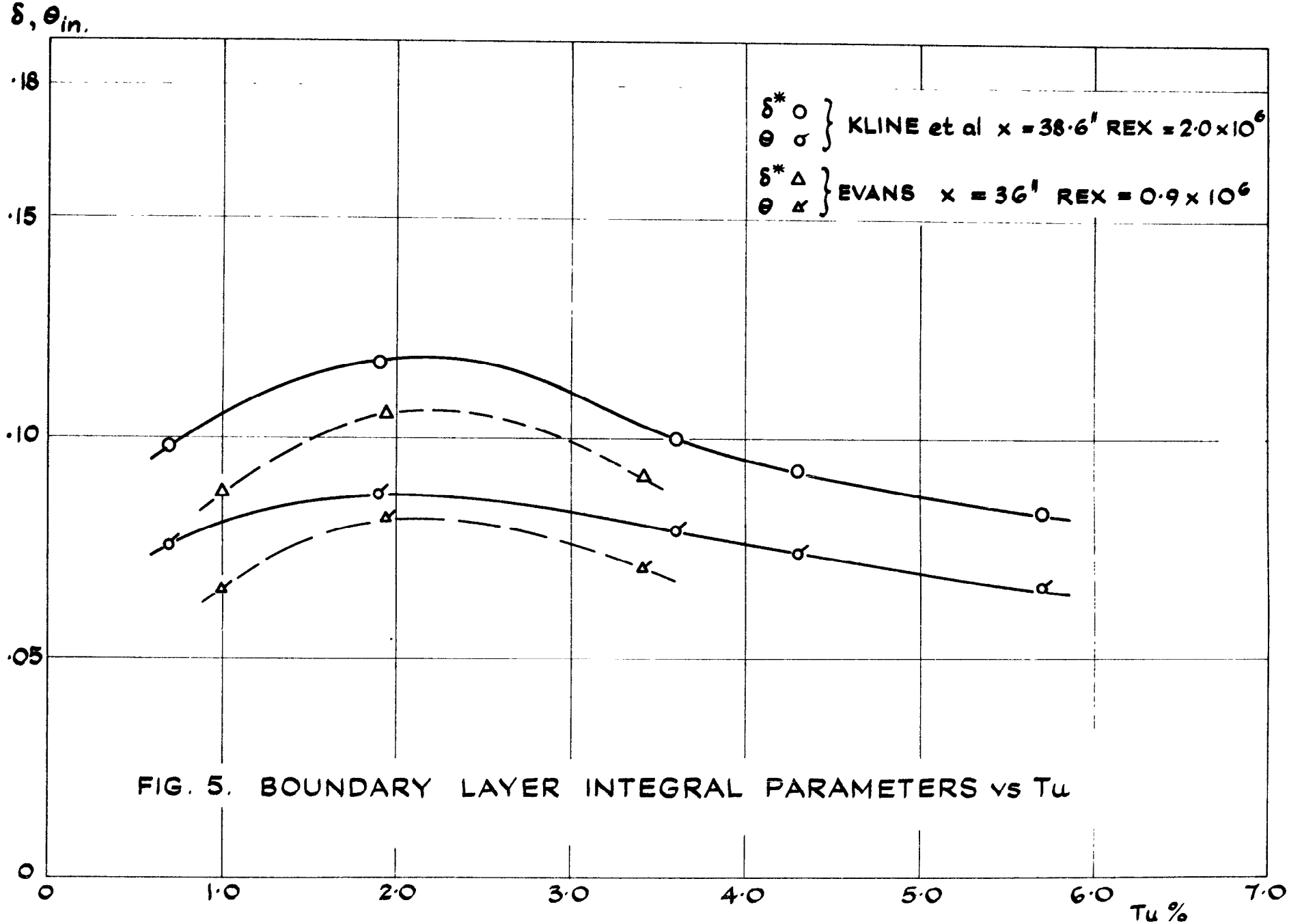

FIG. 5. BOUNDARY LAYER INTEGRAL PARAMETERS vs Tu

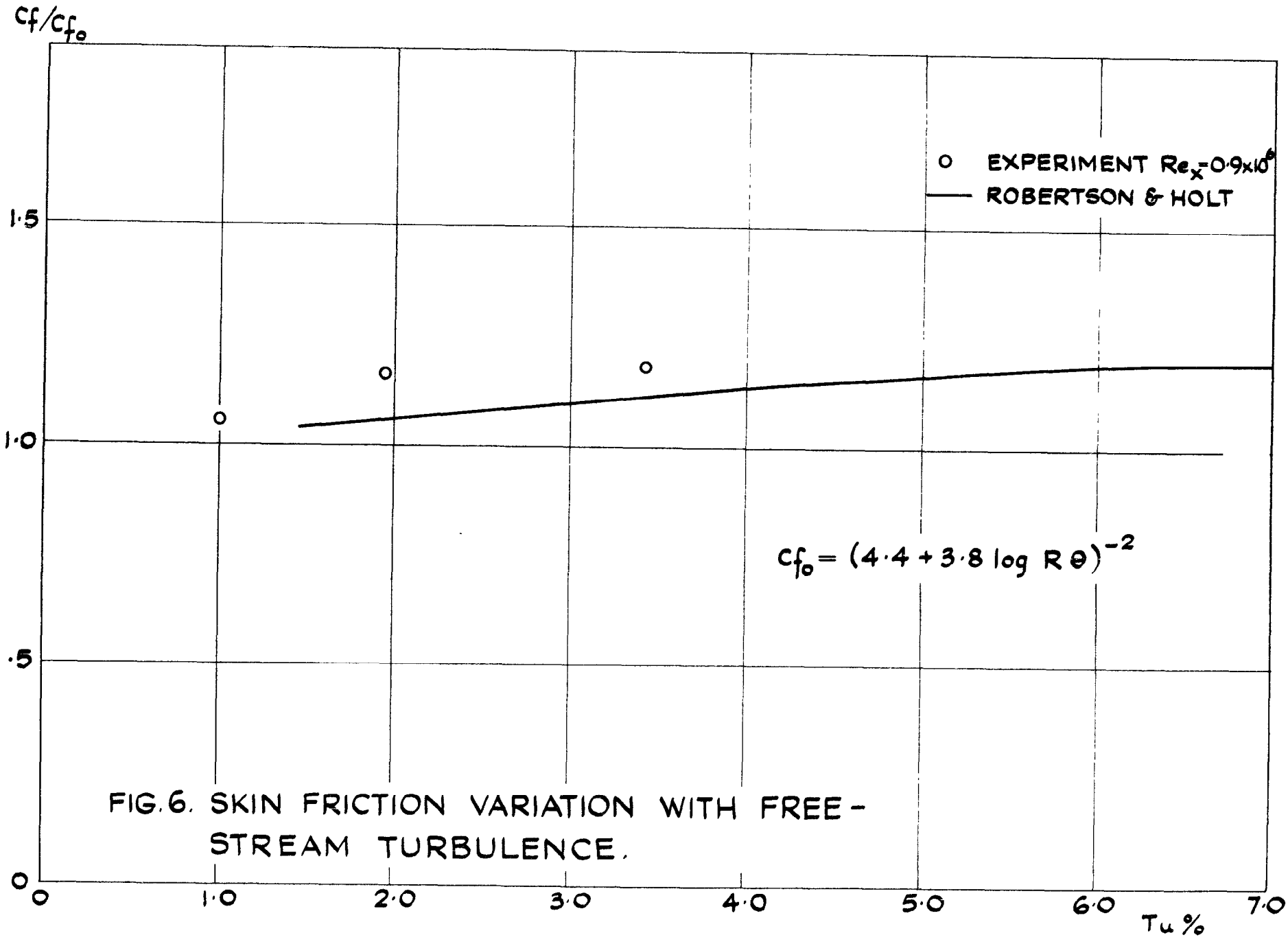

FIG. 6. SKIN FRICTION VARIATION WITH FREE-STREAM TURBULENCE.

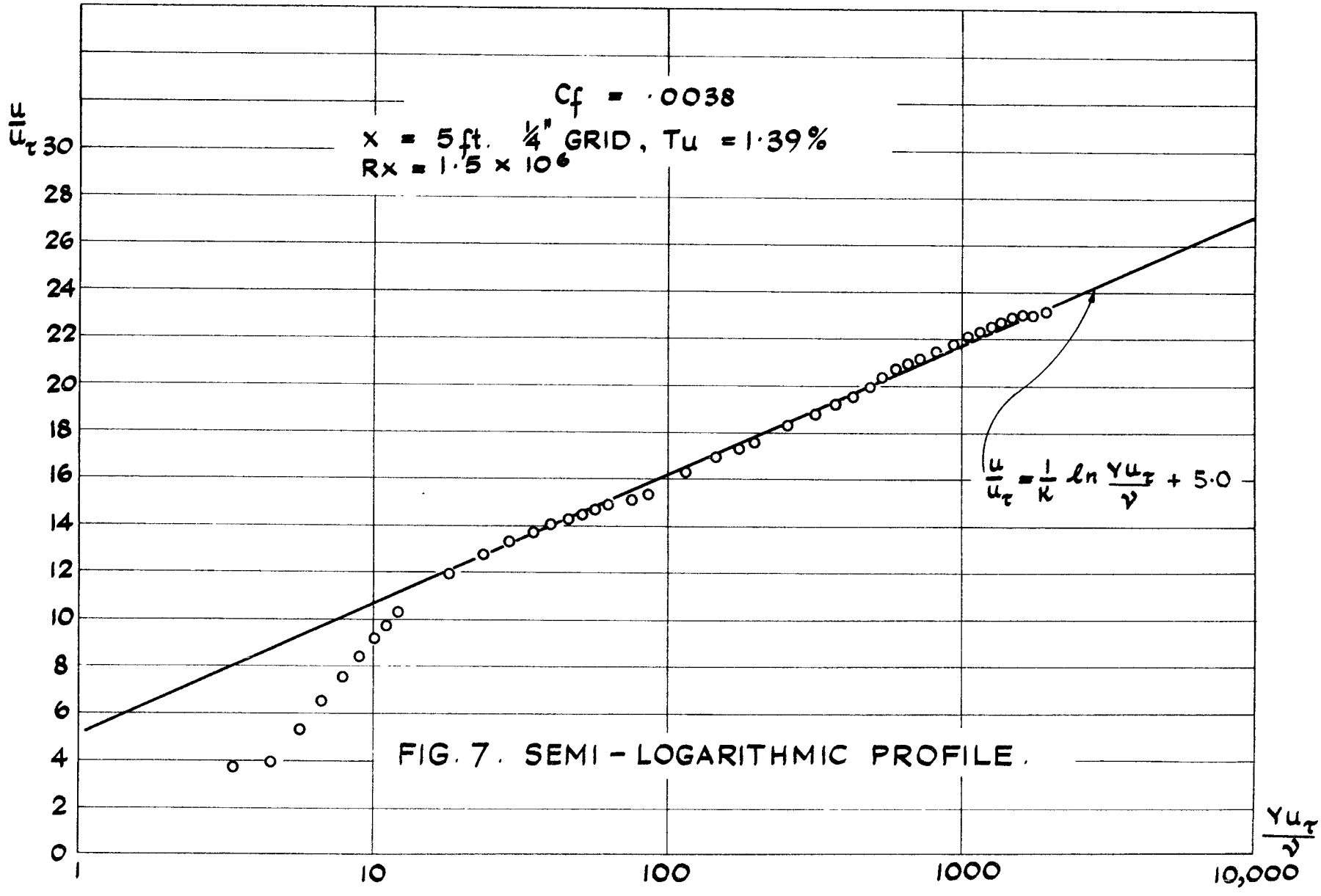

FIG. 7. SEMI - LOGARITHMIC PROFILE.

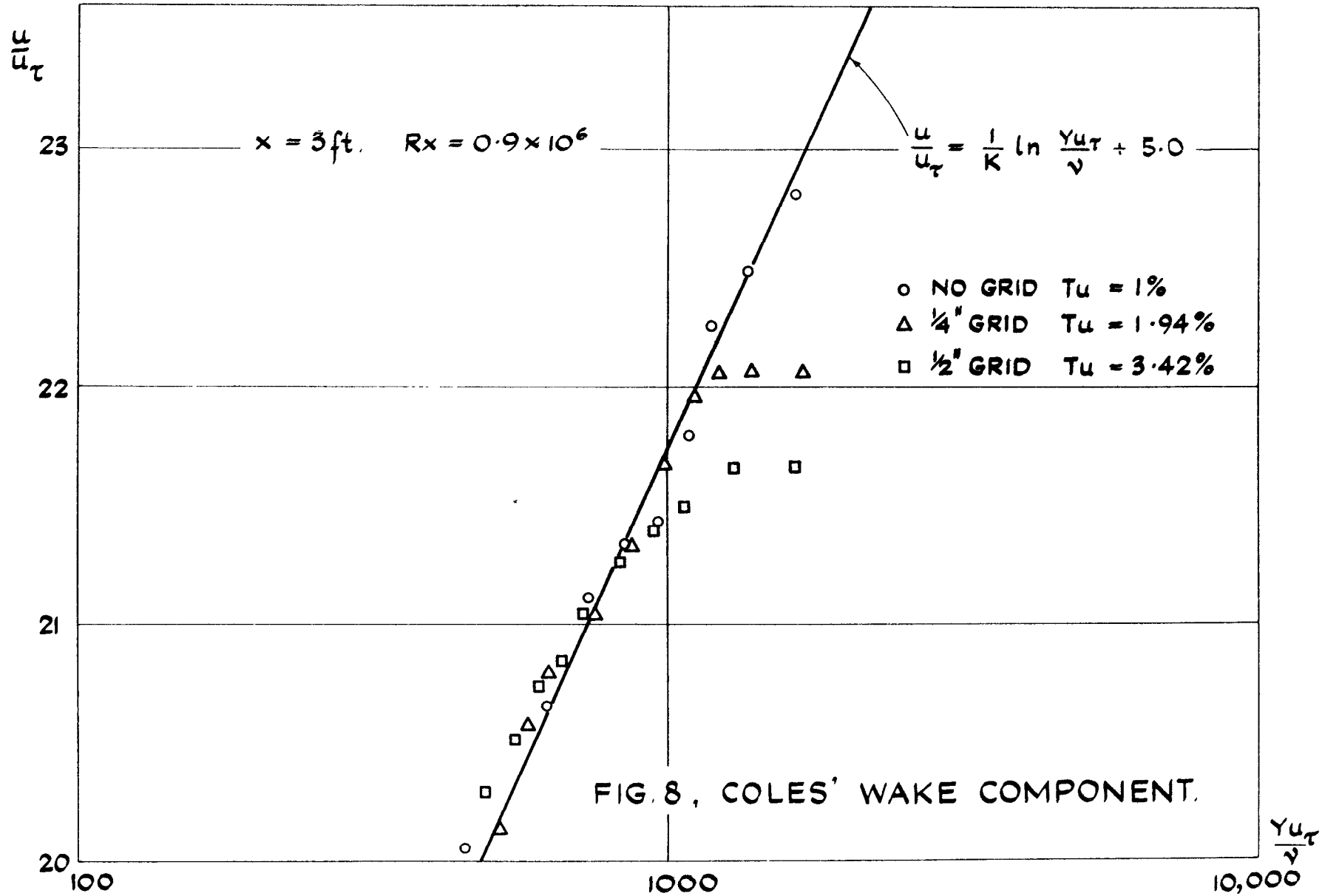

FIG. 8, COLES' WAKE COMPONENT.

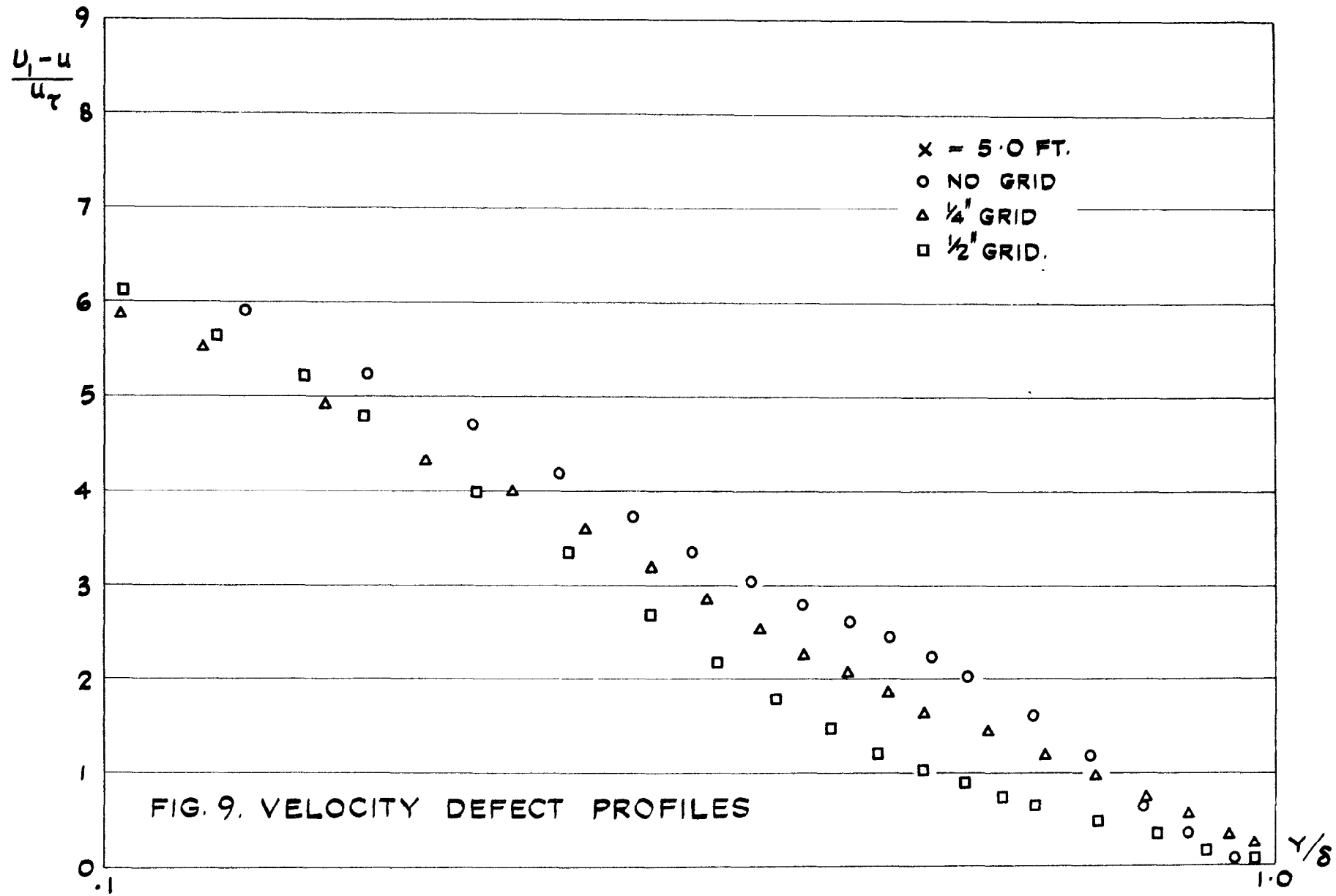

FIG. 9. VELOCITY DEFECT PROFILES

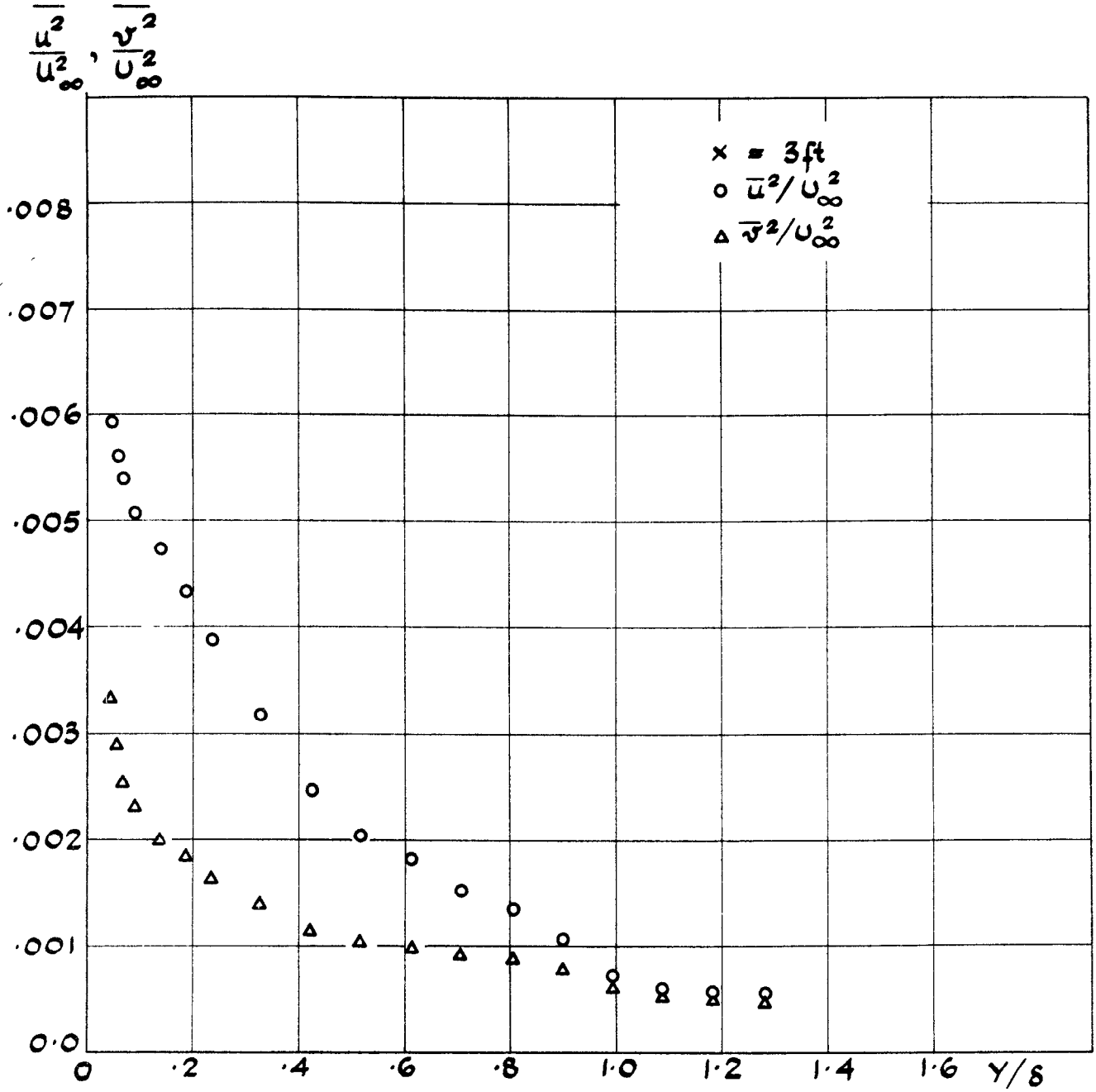

FIG. 10. TURBULENCE INTENSITIES WITH ¼" GRID.

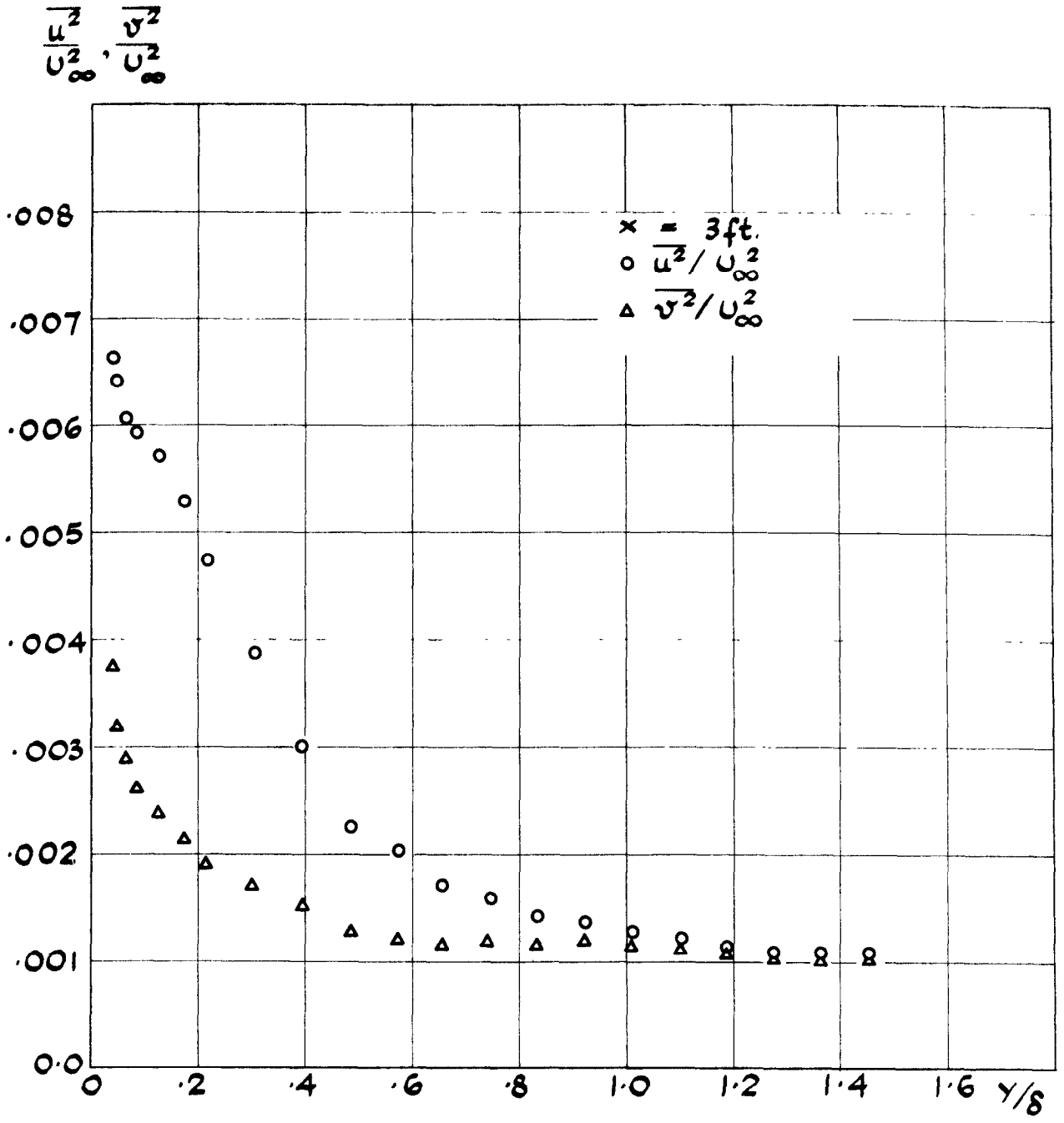

FIG. 11. TURBULENCE INTENSITIES WITH ½" GRID.

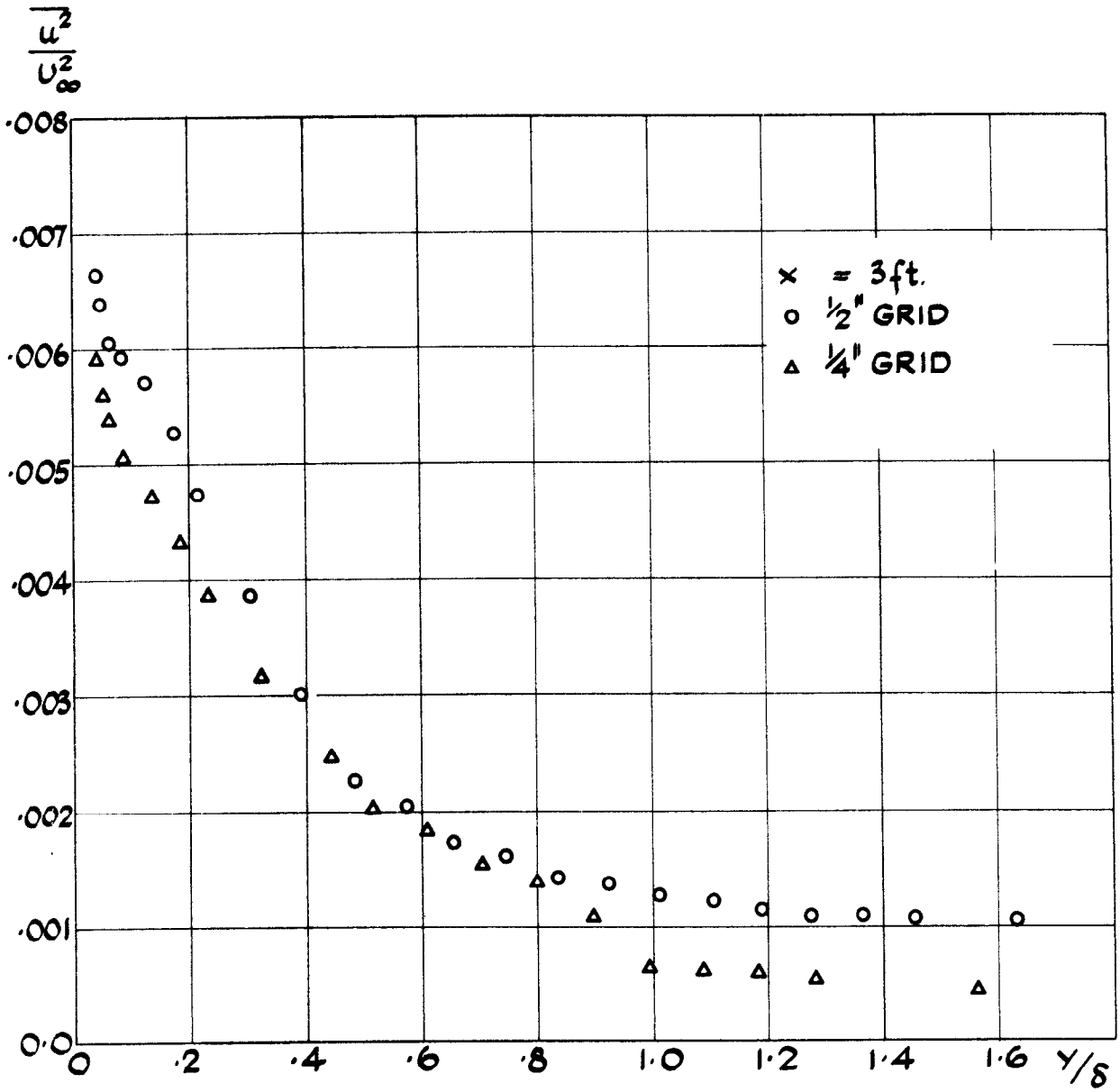

FIG. 12. LONGITUDINAL FLUCTUATING VELOCITY

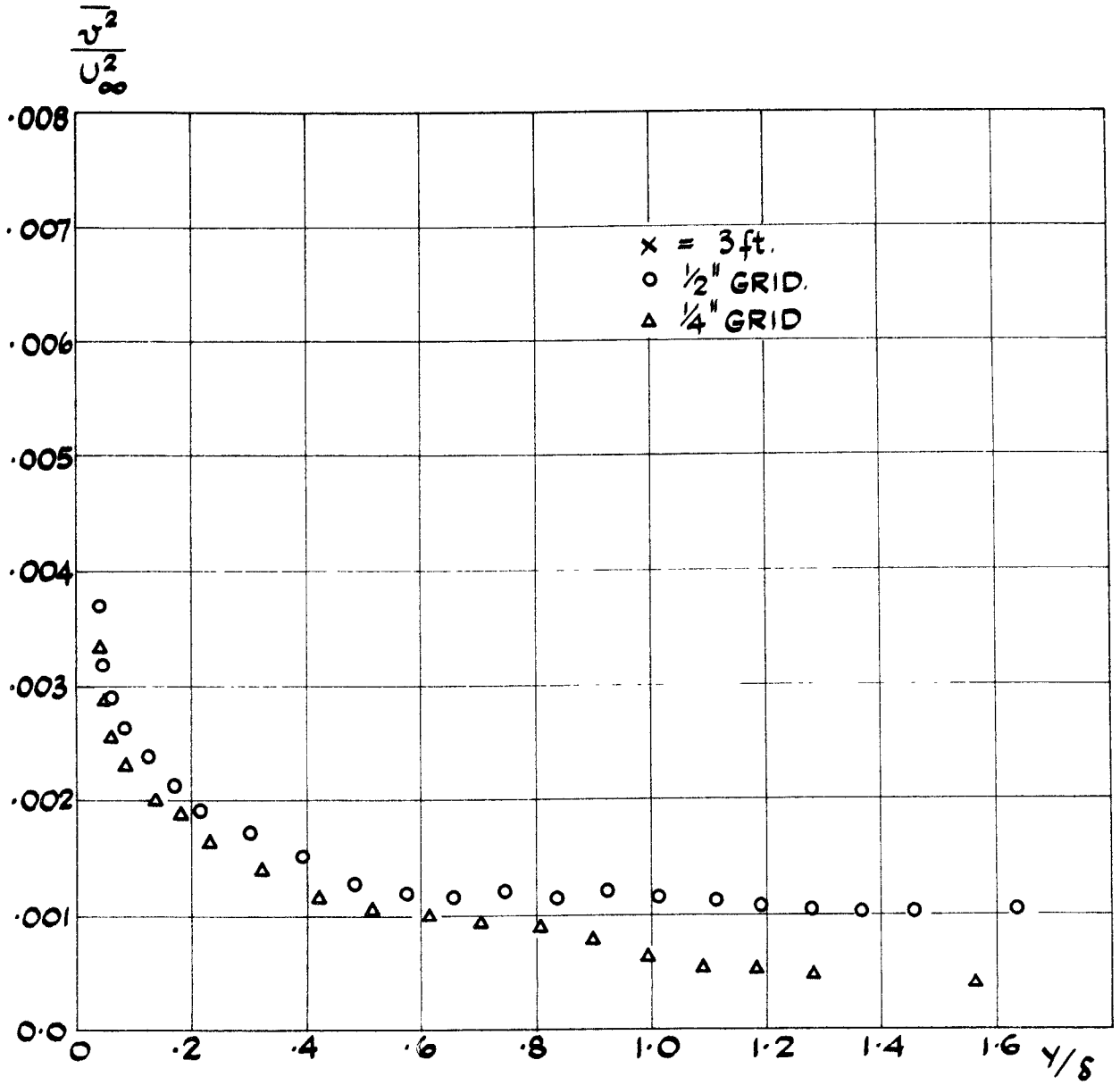

FIG. 13. TRANSVERSE FLUCTUATING VELOCITY.

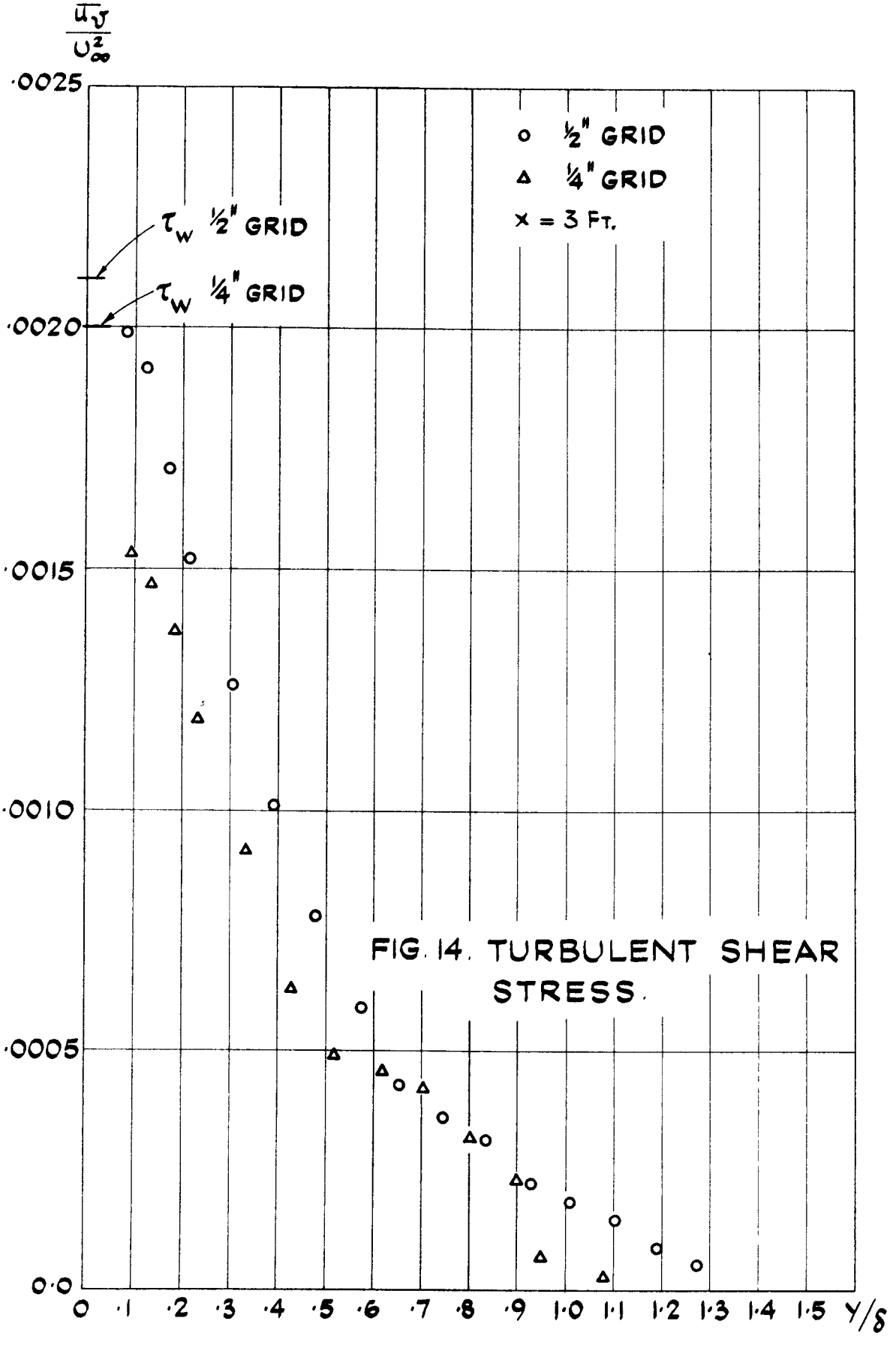

FIG. 14. TURBULENT SHEAR STRESS.

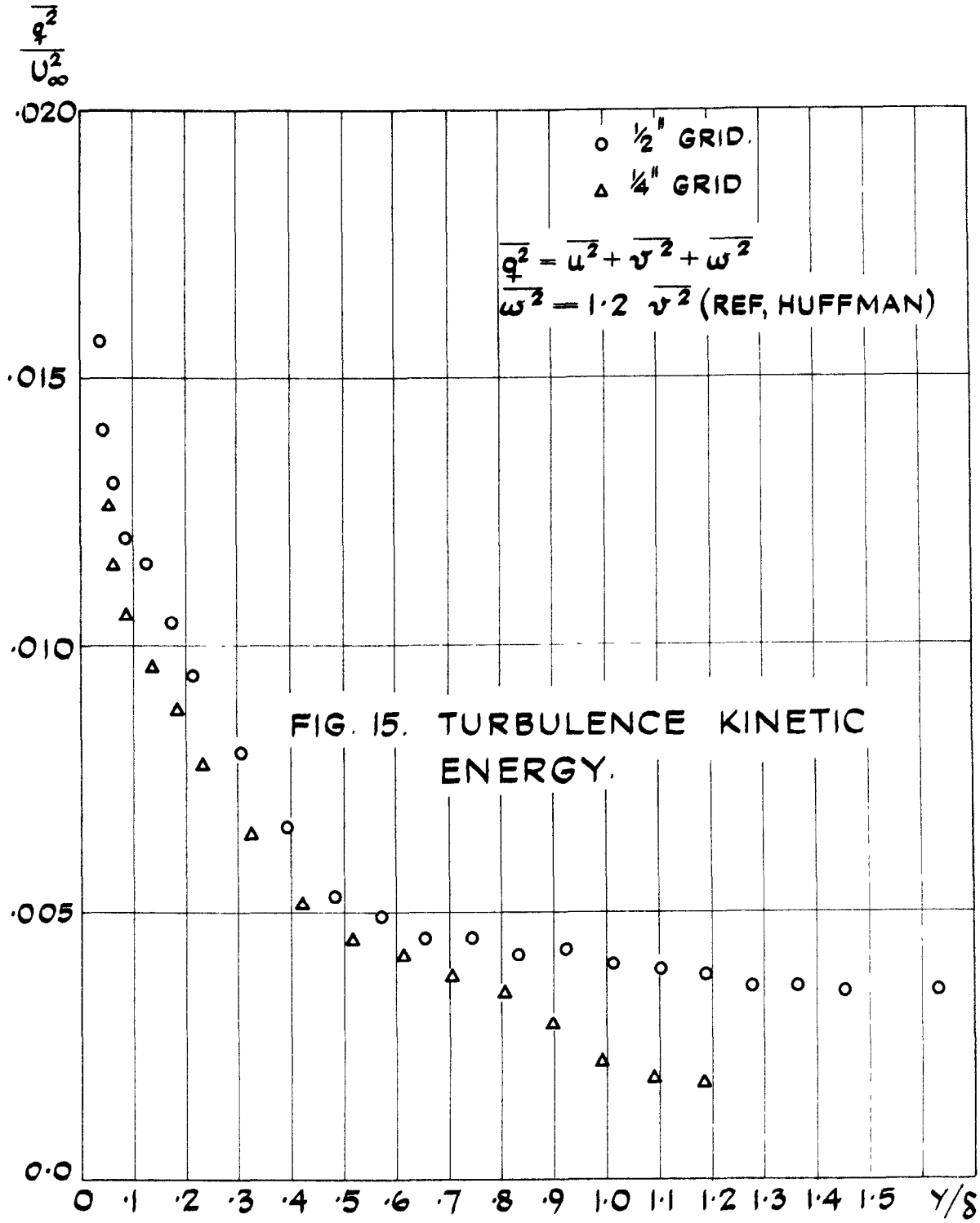

FIG. 15. TURBULENCE KINETIC ENERGY.

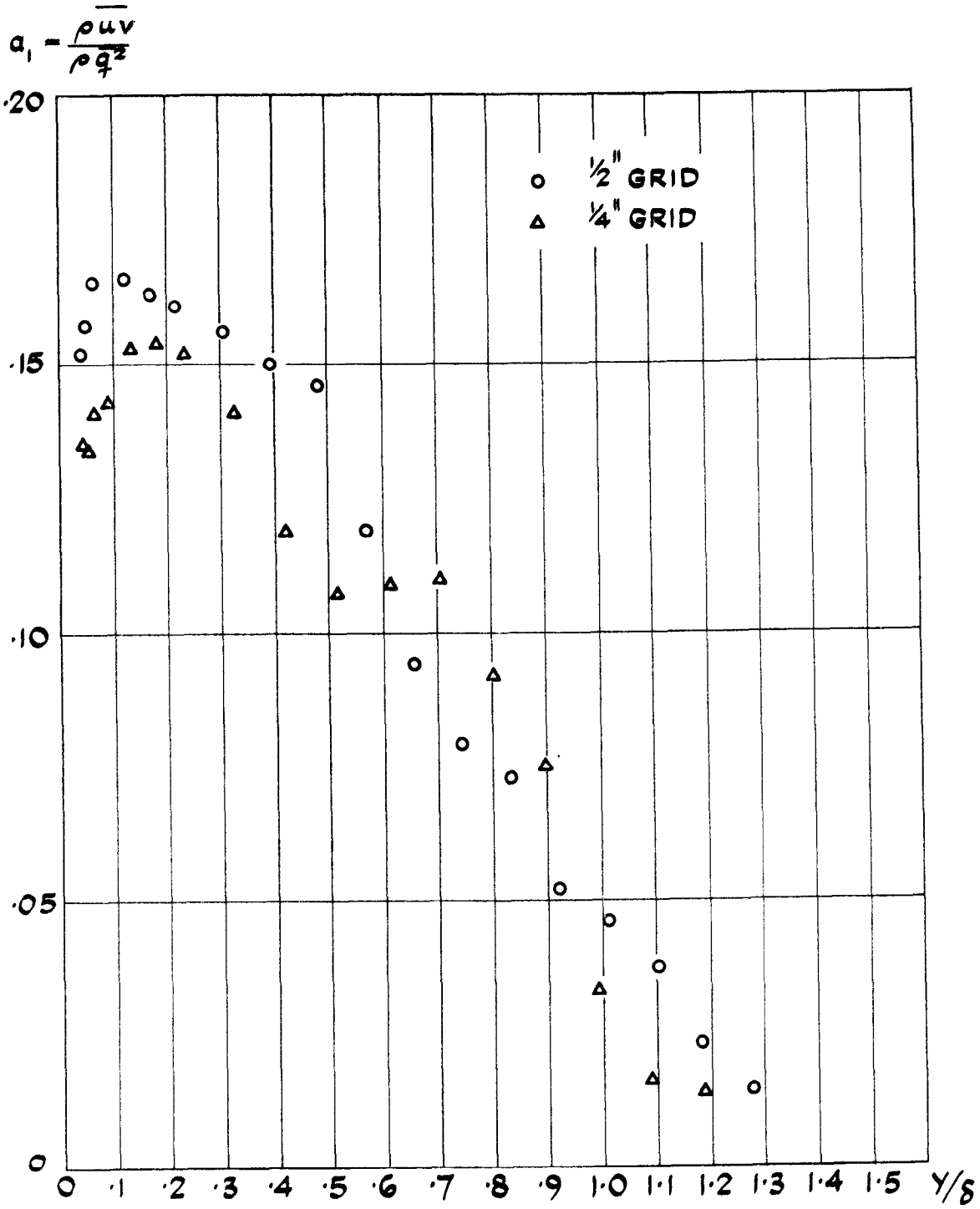

FIG. 16. RATIO OF SHEAR STRESS TO TURBULENCE KINETIC ENERGY.

ARC C.P. No.1282
June, 1973
Evans, R. L.

FREE-STREAM TURBULENCE EFFECTS ON THE TURBULENT BOUNDARY LAYER

The results of an experimental investigation of the effects of free-stream turbulence on a constant pressure turbulent boundary layer are presented. An increase in the fullness of the velocity profile with a consequent decrease in displacement and momentum thickness and an increase in skin friction is found with increasing free-stream turbulence level. Measurements of some of the turbulence structural

properties/

ARC C.P. No.1282
June, 1973
Evans, R. L.

FREE-STREAM TURBULENCE EFFECTS ON THE TURBULENT BOUNDARY LAYER

The results of an experimental investigation of the effects of free-stream turbulence on a constant pressure turbulent boundary layer are presented. An increase in the fullness of the velocity profile with a consequent decrease in displacement and momentum thickness and an increase in skin friction is found with increasing free-stream turbulence level. Measurements of some of the turbulence structural

properties/

ARC C.P. No.1282
June, 1973
Evans, R. L.

FREE-STREAM TURBULENCE EFFECTS ON THE TURBULENT BOUNDARY LAYER

The results of an experimental investigation of the effects of free-stream turbulence on a constant pressure turbulent boundary layer are presented. An increase in the fullness of the velocity profile with a consequent decrease in displacement and momentum thickness and an increase in skin friction is found with increasing free-stream turbulence level. Measurements of some of the turbulence structural

properties/

properties show an increase in the turbulence kinetic energy and the turbulent shear stress throughout the boundary layer with increasing free-stream turbulence.

The turbulent shear stress, $-\rho\overline{uv}$, was found to persist into the free-stream, well beyond the usual $\delta_{.99}$ edge of the boundary layer.

properties show an increase in the turbulence kinetic energy and the turbulent shear stress throughout the boundary layer with increasing free-stream turbulence.

The turbulent shear stress, $-\rho\overline{uv}$, was found to persist into the free-stream, well beyond the usual $\delta_{.99}$ edge of the boundary layer.

properties show an increase in the turbulence kinetic energy and the turbulent shear stress throughout the boundary layer with increasing free-stream turbulence.

The turbulent shear stress, $-\rho\overline{uv}$, was found to persist into the free-stream, well beyond the usual $\delta_{.99}$ edge of the boundary layer.

HER MAJESTY'S STATIONERY OFFICE

Government Bookshops

49 High Holborn, London WC1V 6HB
13a Castle Street, Edinburgh EH2 3AR
41 The Hayes, Cardiff CF1 1JW
Brazennose Street, Manchester M60 8AS
Southey House, Wine Street, Bristol BS1 2BQ
258 Broad Street, Birmingham B1 2HE
80 Chichester Street, Belfast BT1 4JY

Government publications are also available through booksellers

C.P. No. 1282

ISBN 011 470866 5